PT-JPL EVAPOTRANSPIRATION

REMOTE SENSING DEVELOPMENTS AT NASA'S JET PROPULSION LABORATORY

DR. JOSHUA B. FISHER

MANISH VERMA | KANISKA MALLICK | KEVIN TU | YOUNGRYEL RYU | ALEXANDRE GUILLAUME | GREGORY MOORE | MUNISH SIKKA | LAVANYA RAMAKRISHNAN | VALERIE HENDRIX

WATER & CARBON CYCLES GROUP
NASA JET PROPULSION LABORATORY (JPL)
CALIFORNIA INSTITUTE OF TECHNOLOGY (CALTECH)

JOINT INSTITUTE FOR REGIONAL EARTH SYSTEM SCIENCE & ENGINEERING
UNIVERSITY OF CALIFORNIA, LOS ANGELES (UCLA)

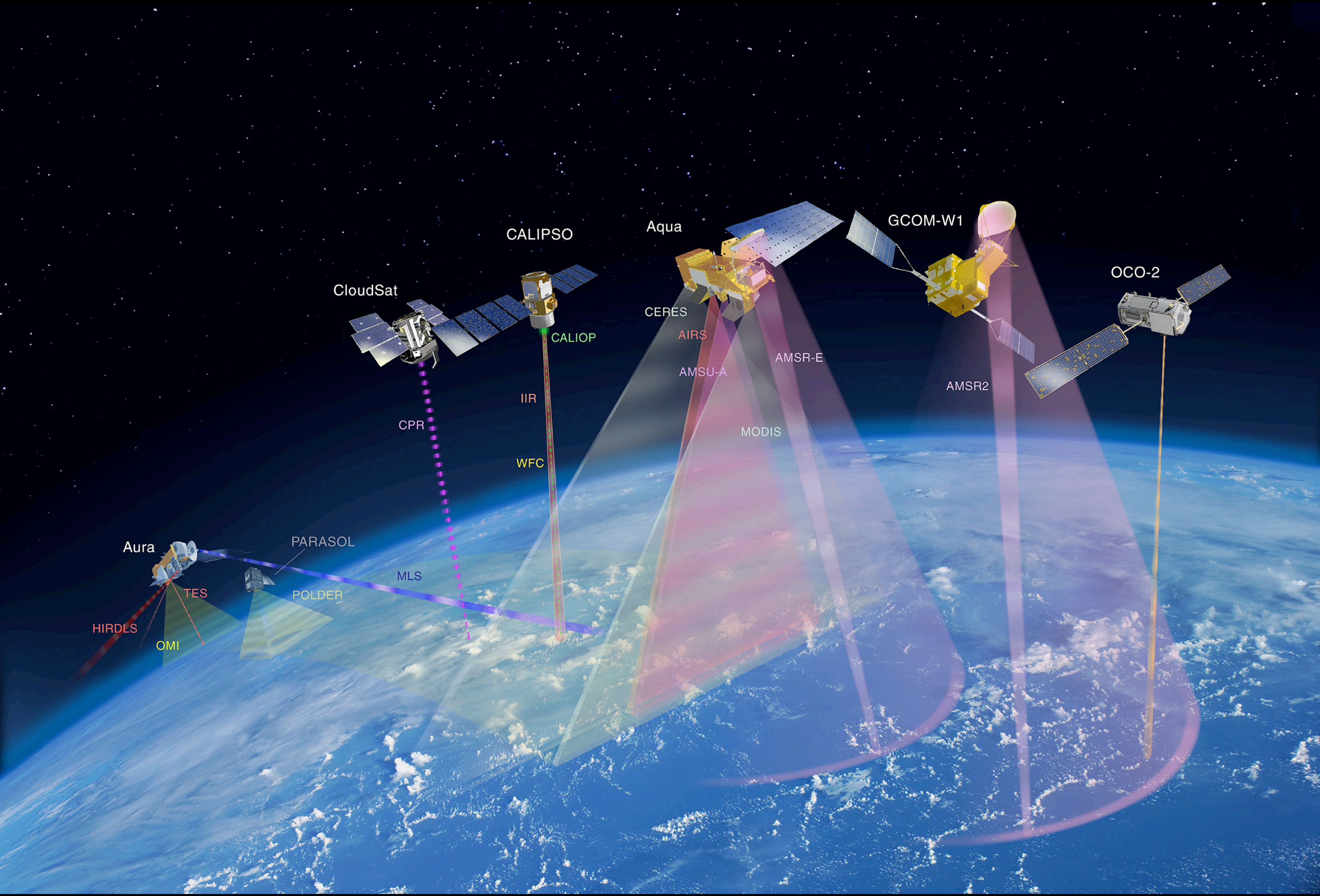
CALIPSO
Aqua
GCOM-W1
CloudSat
OCO-2
CERES
CALIOP
AIRS
AMSR-E
AMSU-A
AMSR2
IIR
CPR
MODIS
WFC
Aura
PARASOL
MLS
TES
POLDER
HIRDLS
OMI

JPL EVAPOTRANSPIRATION (PT-JPL)

Global estimates of the land–atmosphere water flux based on monthly AVHRR and ISLSCP-II data, validated at 16 FLUXNET sites

JB **Fisher**, KP Tu, DD Baldocchi - Remote Sensing of Environment, **2008** - Elsevier

Numerous models of evapotranspiration have been published that range in data-driven complexity, but global estimates require a model that does not depend on intensive field measurements. The Priestley–Taylor model is relatively simple, and has proven to be **...**

Cited by 164   Related articles   All 11 versions   Cite   Save

PT-JPL ET

1/3

$$LE_{pot} = \alpha \frac{\Delta}{\Delta + \gamma} R_n$$

Priestley & Taylor (1972)

Fisher, J.B., et al., 2008: *Remote Sensing of Environment*.

PT-JPL ET

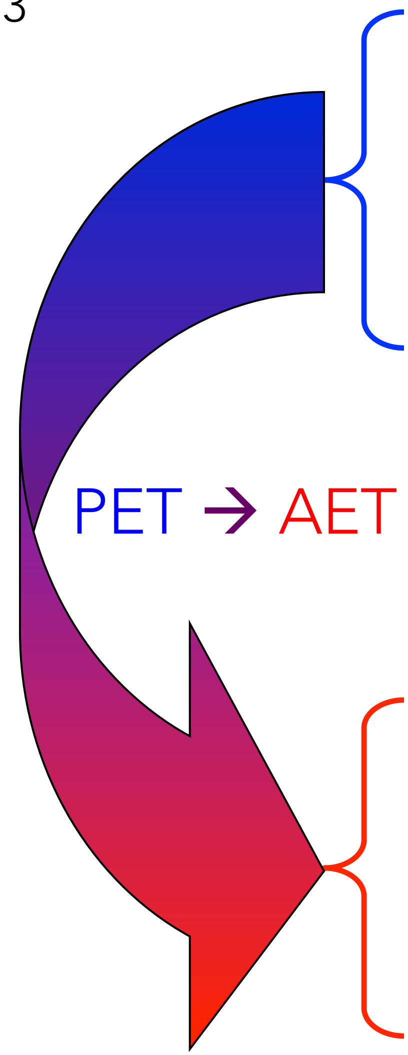

$$LE_{pot,canopy} = (1 - f_{wet})\alpha \frac{\Delta}{\Delta + \gamma} R_{nc}$$

$$LE_{pot,soil} = (1 - f_{wet})\alpha \frac{\Delta}{\Delta + \gamma} R_{ns}$$

$$LE_{pot,interception} = f_{wet}\alpha \frac{\Delta}{\Delta + \gamma} R_{n}$$

PT-JPL ET

3/3

$$LE_c = (1 - f_{wet}) f_g f_T f_M \alpha \frac{\Delta}{\Delta + \gamma} R_{nc}$$

$$LE_s = (f_{wet} + f_{SM}(1 - f_{wet}))\alpha \frac{\Delta}{\Delta + \gamma} (R_{ns} - G)$$

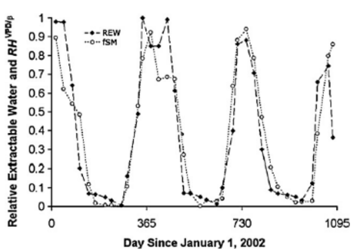

Fig. 1. Comparison of monthly f_{SM} to normalized volumetric water content (VWC), or relative extractable water – REW = (VWC − VWC_{min})/(VWC_{max} − VWC_{min}) – at an oak–savanna site.

PT-JPL ET

$$LE = LE_s + LE_c + LE_i$$

Net Radiation	MODIS | CERES | SRB | ISCCP
Air Temperature	MODIS | AIRS
Relative Humidity	MODIS | AIRS
Vegetation fraction	MODIS | Landsat

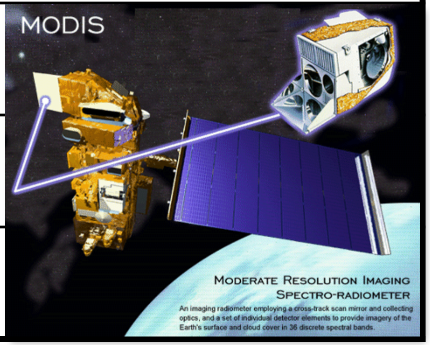

JPL MODIS R_n

$$R_n = (1 - albedo) * SW_{dn} + LW_{dn} - LW_{up}$$

- *We combined 11 variables from 6 different MODIS products daily over the MODIS era to estimate the components of R_n.*

Component of R_n	MODIS products and method
Albedo	Albedo from **MCD43** (500 m, 8-day), land cover from **MCD12** (500 m, annual)
Incoming Shortwave (SW_{dn})	Cloud optical thickness, cloud top altitude, and solar zenith angle from **MOD06** (5 km, daily); aerosol optical thickness at 550 nm from **MOD04** (10 km, daily); Input MODIS data to a radiative transfer model (Kobayashi et al., 2008)
Incoming Longwave (LW_{dn})	Near surface air temperature and vapor pressure from **MOD07** (5 km, daily); estimate emissivity from vapor pressure and temperature
Outgoing Longwave (LW_{up})	Land surface temperature and emissivity from **MOD11** (1 km, daily); estimate broadband emissivity

JPL MODIS R_n

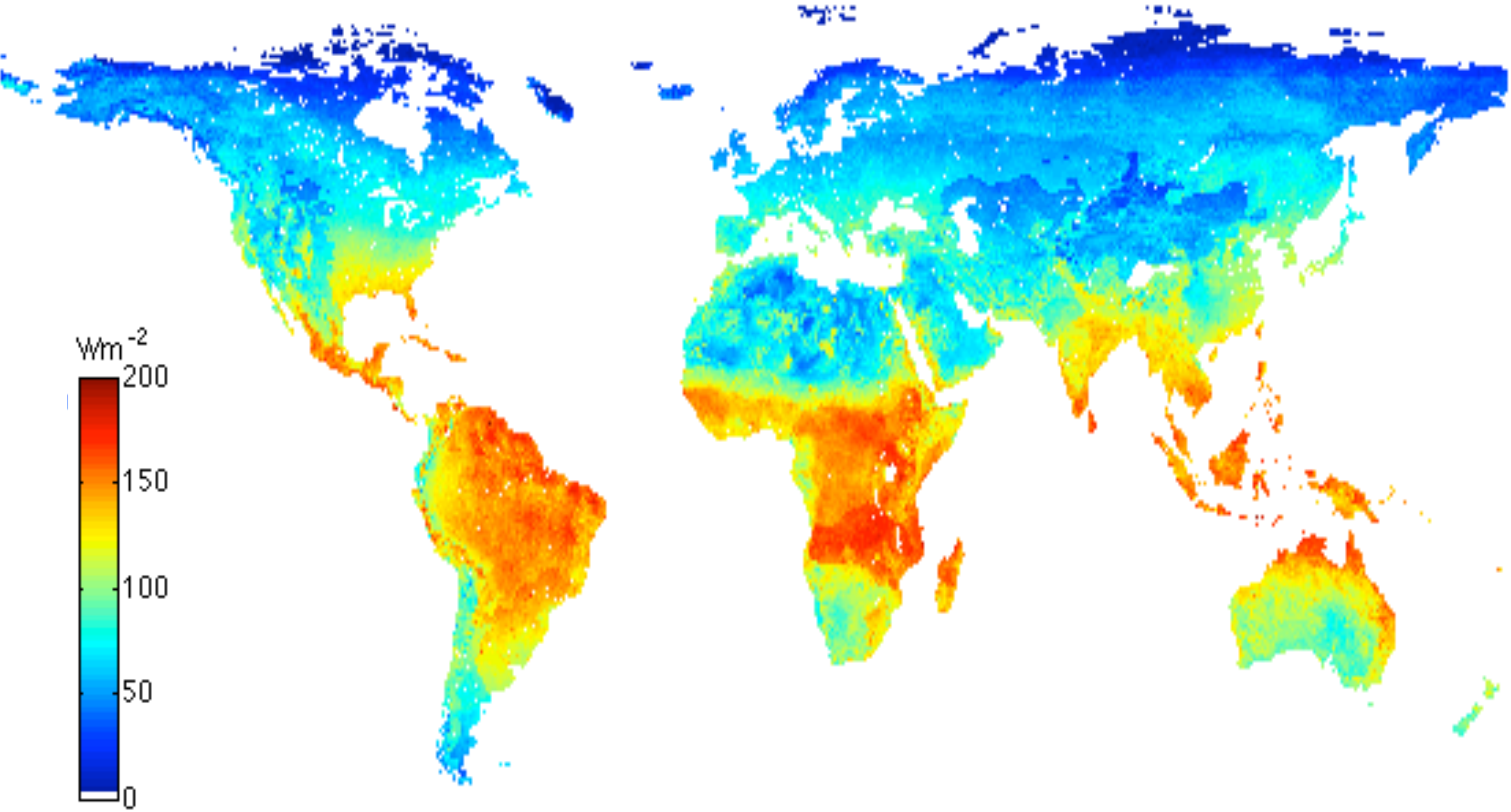

JPL MODIS R_n

- *Validation at 126 sites across FLUXNET and SURFRAD.*

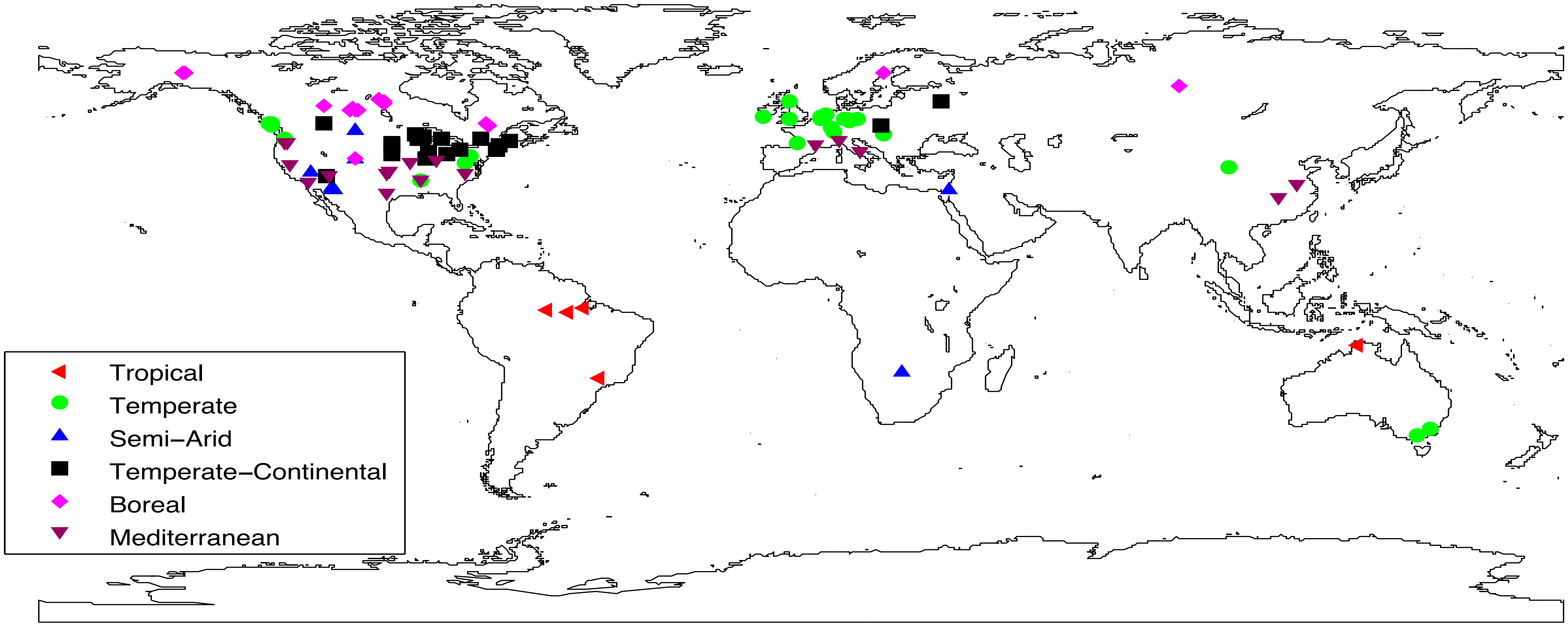

JPL MODIS R_n

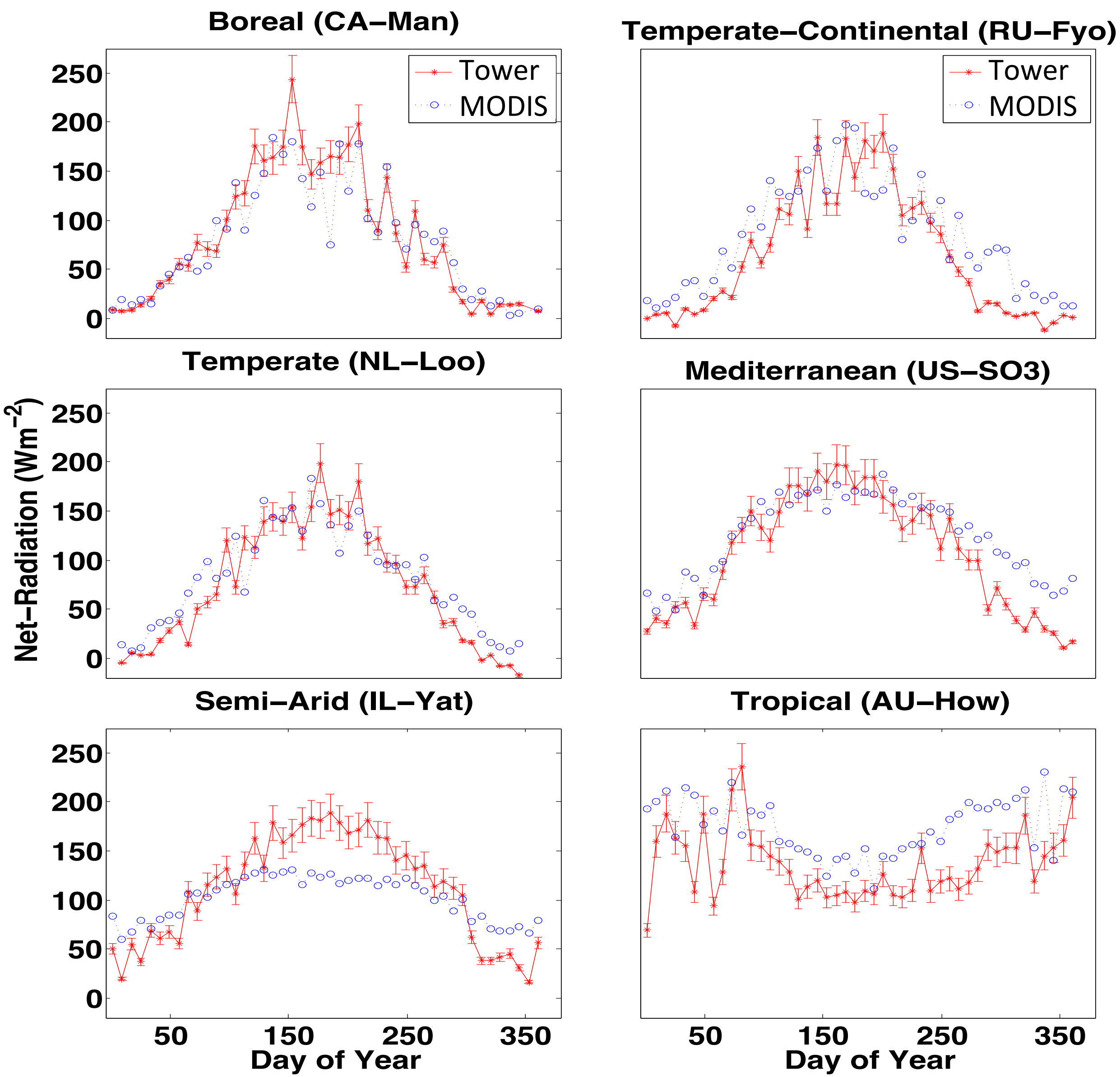

Boreal (CA–Man)
Temperate–Continental (RU–Fyo)
Temperate (NL–Loo)
Mediterranean (US–SO3)
Semi–Arid (IL–Yat)
Tropical (AU–How)
Tower
MODIS
Net–Radiation (Wm^{-2})
Day of Year
0
50
100
150
200
250
350

JPL MODIS R_n

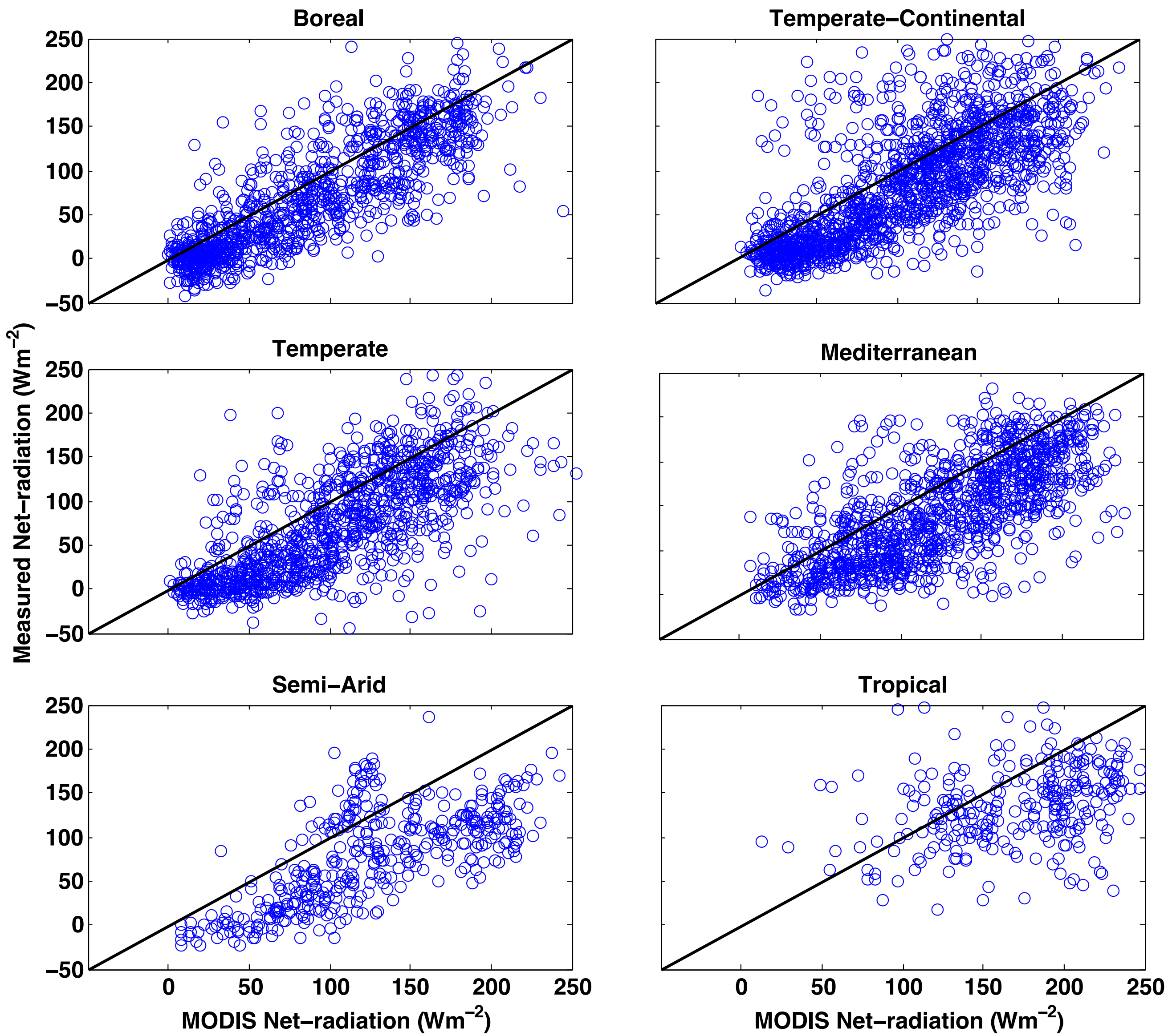

Boreal
Temperate–Continental
Temperate
Mediterranean
Semi–Arid
Tropical
Measured Net–radiation (Wm^{-2})
MODIS Net–radiation (Wm^{-2})
250
200
150
100
50
0
−50

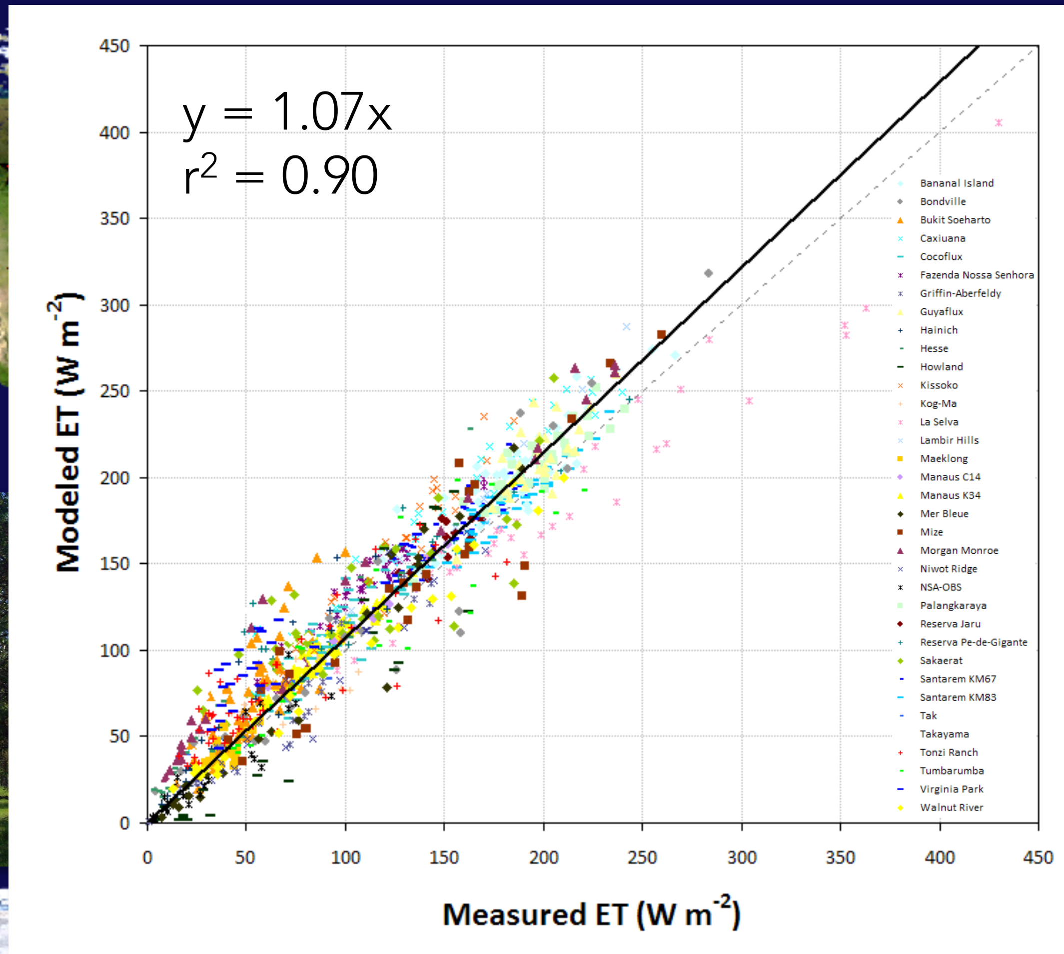

PT-JPL ET VALIDATION

PT-JPL ET VALIDATION

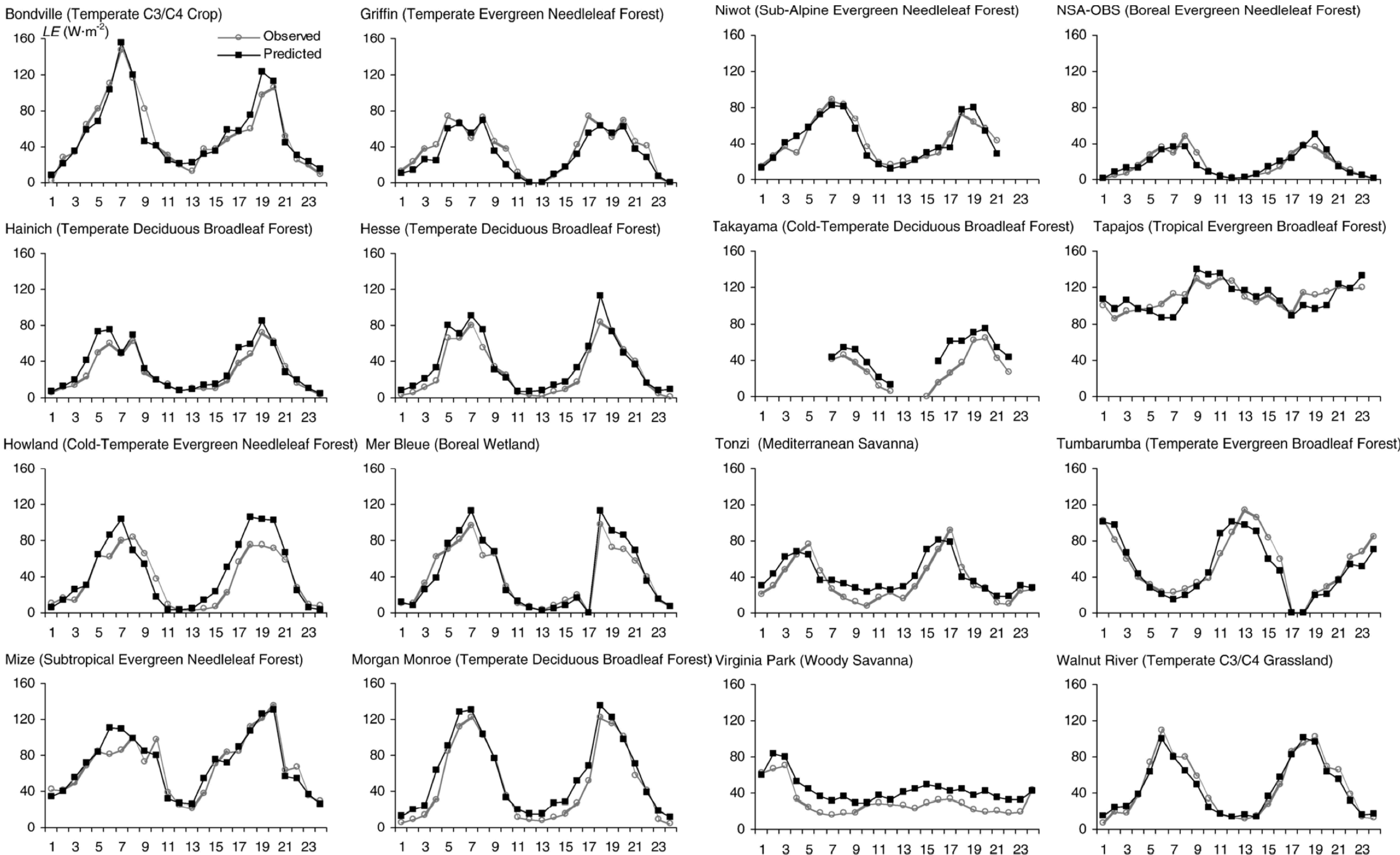

INDEPENDENT EVALUATION (GEWEX/PRINCETON)

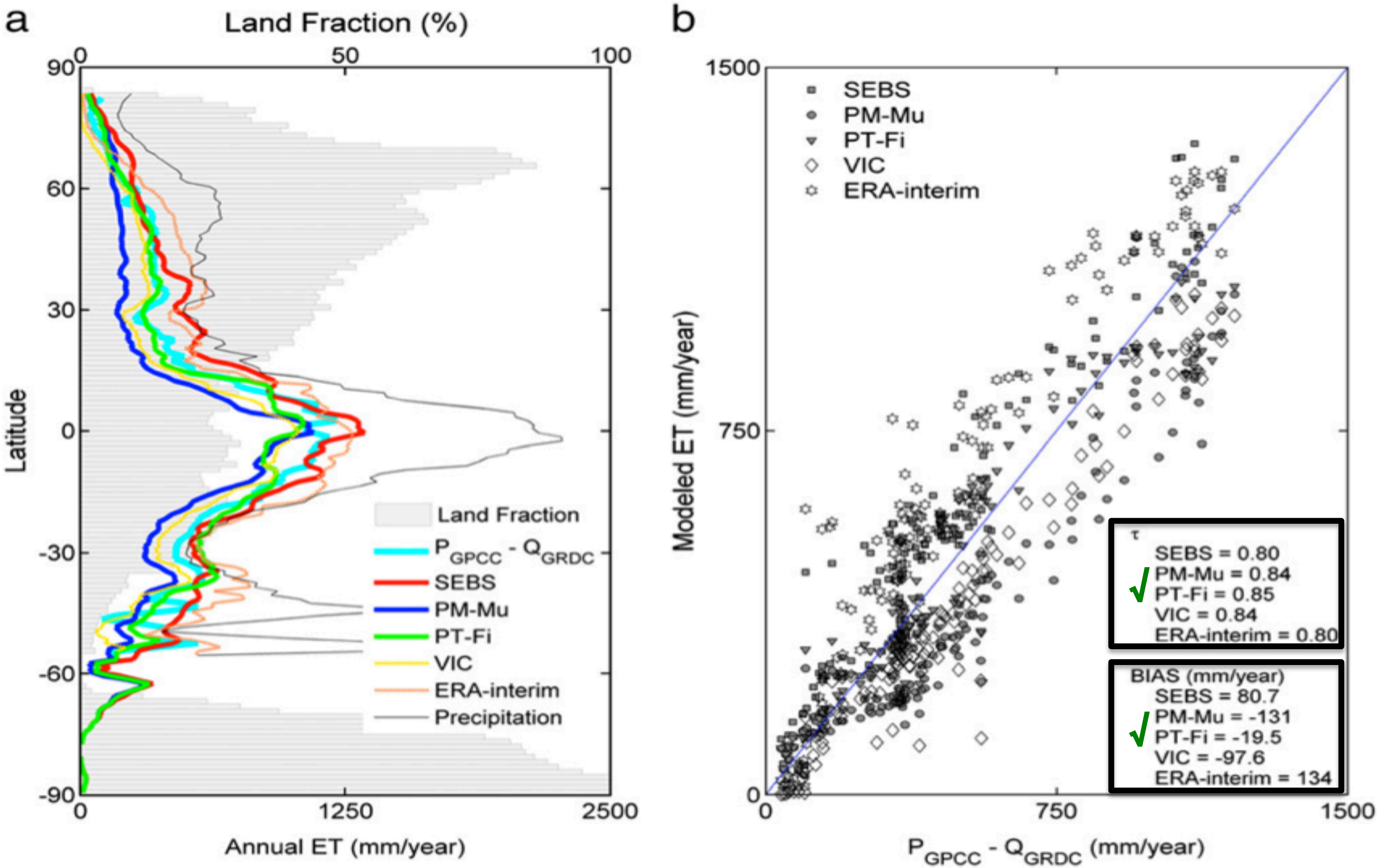

Vinukollu et al. 2011: *Remote Sensing of Environment*

INDEPENDENT EVALUATION (BEIJING)

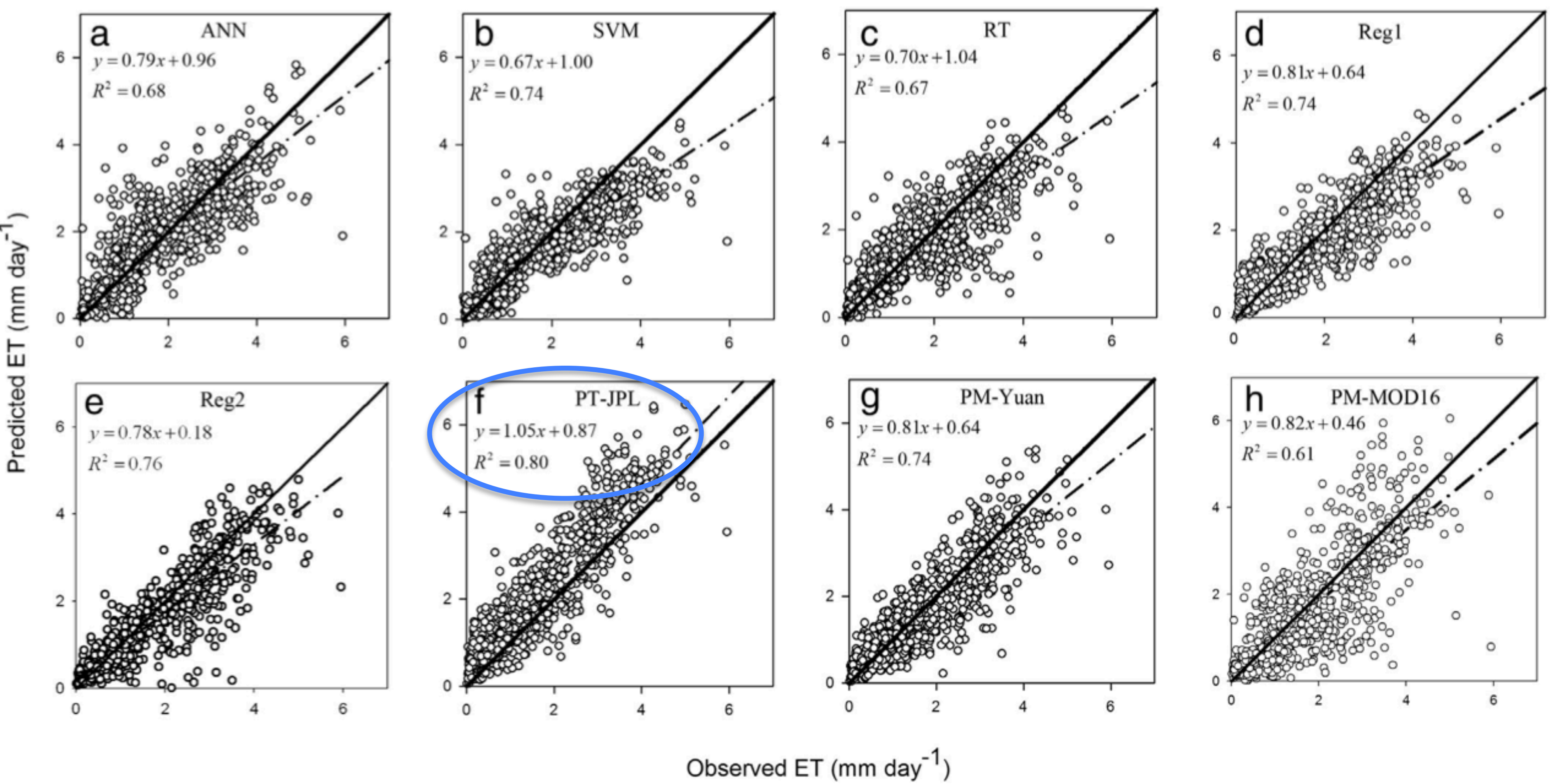

Chen et al. 2014: *Remote Sensing of Environment*

INDEPENDENT EVALUATION (GEWEX/AUSTRALIA)

Agricultural and Forest Meteorology 187 (2014) 46–61

Contents lists available at ScienceDirect

Agricultural and Forest Meteorology

journal homepage: www.elsevier.com/locate/agrformet

Multi-site evaluation of terrestrial evaporation models using FLUXNET data

A. Ershadi[a,*], M.F. McCabe[b], J.P. Evans[c,d], N.W. Chaney[e], E.F. Wood[e]

[a] School of Civil & Environmental Engineering, University of NSW, Sydney, NSW, Australia
[b] Water Desalination and Reuse Centre, King Abdullah University of Science and Technology (KAUST), Jeddah, Saudi Arabia
[c] ARC Centre of Excellence for Climate Systems Science, University of NSW, Sydney, Australia
[d] Climate Change Research Centre, University of NSW, Sydney, Australia
[e] Department of Civil and Environmental Engineering, Princeton University, Princeton, NJ, USA

A R T I C L E I N F O

Article history:
Received 3 March 2013
Received in revised form 5 October 2013
Accepted 23 November 2013

Keywords:
Multi-model intercomparison
Latent heat flux
Energy balance
Penman–Monteith
Advection-aridity
Priestley–Taylor

A B S T R A C T

We evaluated the performance of four commonly applied land surface evaporation models using a high-quality dataset of selected FLUXNET towers. The models that were examined include an energy balance approach (Surface Energy Balance System; SEBS), a combination-type technique (single-source Penman–Monteith; PM), a complementary method (advection-aridity; AA) and a radiation based approach (modified Priestley–Taylor; PT-JPL). Twenty FLUXNET towers were selected based upon satisfying stringent forcing data requirements and representing a wide range of biomes. These towers encompassed a number of grassland, cropland, shrubland, evergreen needleleaf forest and deciduous broadleaf forest sites. Based on the mean value of the Nash–Sutcliffe efficiency (*NSE*) and the root mean squared difference (*RMSD*), the order of overall performance of the models from best to worst were: ensemble mean of models (0.61, 64), PT-JPL (0.59, 66), SEBS (0.42, 84), PM (0.26, 105) and AA (0.18, 105) [statistics stated as (*NSE*, *RMSD* in $\mathrm{W\,m^{-2}}$)]. Although PT-JPL uses a relatively simple and largely empirical formulation of the evaporative process, the technique showed improved performance compared to PM, possibly due to its partitioning of total evaporation (canopy transpiration, soil evaporation, wet canopy evaporation) and lower uncertainties in the required forcing data. The SEBS model showed low performance over tall and heterogeneous canopies, which was likely a consequence of the effects of the roughness sub-layer parameterization employed in this scheme. However, SEBS performed well overall. Relative to PT-JPL and SEBS, the PM and AA showed low performance over the majority of sites, due to their sensitivity to the parameterization of resistances. Importantly, it should be noted that no single model was consistently best across all biomes. Indeed, this outcome highlights the need for further evaluation of each model's structure and parameterizations to identify sensitivities and their appropriate application to different surface types and conditions. It is expected that the results of this study can be used to inform decisions regarding model choice for water resources and agricultural management, as well as providing insight into model selection for global flux monitoring efforts.

1. Introduction

Reliable estimates of evaporation (E) are required for the accurate representation of mass and energy exchanges at the land surface. In hydrological and water resource studies, an evaporation model is required to characterize the exchange of moisture between the surface and the overlying atmosphere. Not surprisingly, the choice of model can have considerable impact on water resource planning and decision support across a range of temporal and spatial scales. Improved understanding of the influence of model choice on flux estimation is required in order to better characterize the fidelity of these simulations, particularly in light of an increasing number of regional and global scale efforts to produce land surface heat flux data products (Jiménez et al., 2011; Mueller et al., 2013).

A number of models have been developed for the estimation of either the reference, potential or actual values of evaporation (see reviews of Kalma et al., 2008 and Wang and Dickinson, 2012). The reference evaporation is defined as the evaporation from a hypothetical, well-watered 'reference' crop (Allen, 2000), while potential evaporation is the maximum evaporation for a given surface if moisture is not limiting (Penman, 1948; Irmak and Haman, 2003). Estimation of the reference and potential evaporation is

* Corresponding author. Tel.: +61 403053522.
E-mail addresses: a.ershadi@studnet.unsw.edu.au (A. Ershadi), matthew.mccabe@kaust.edu.sa (M.F. McCabe), jason.evans@unsw.edu.au (J.P. Evans), nchaney@princeton.edu (N.W. Chaney), efwood@princeton.edu (E.F. Wood).

0168-1923/$ – see front matter
http://dx.doi.org/10.1016/j.agrformet.2013.11.008

PT-JPL was the best performing ET retrieval algorithm.

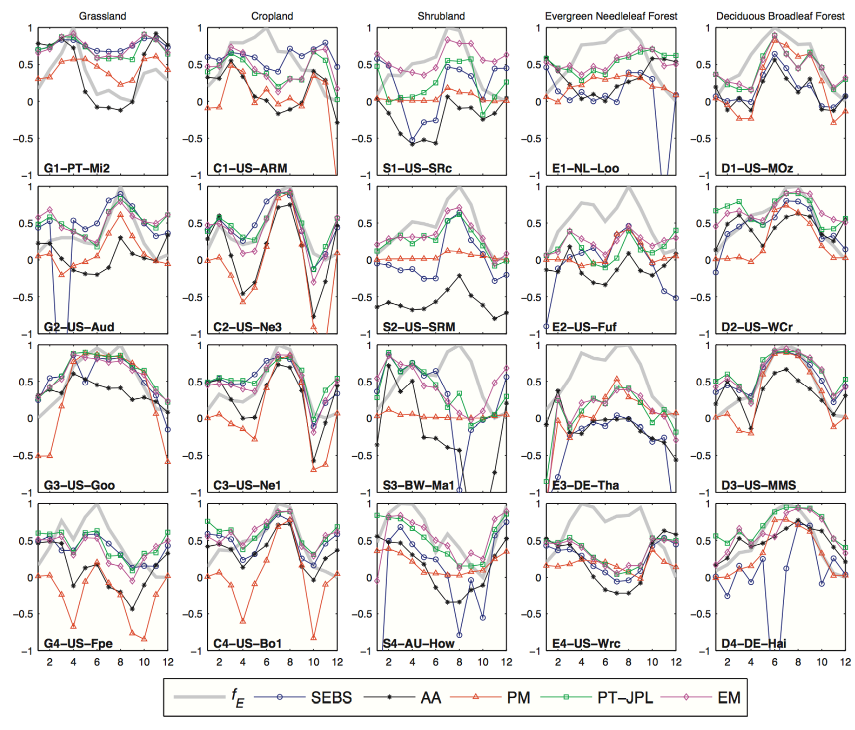

PT-JPL GLOBAL ET

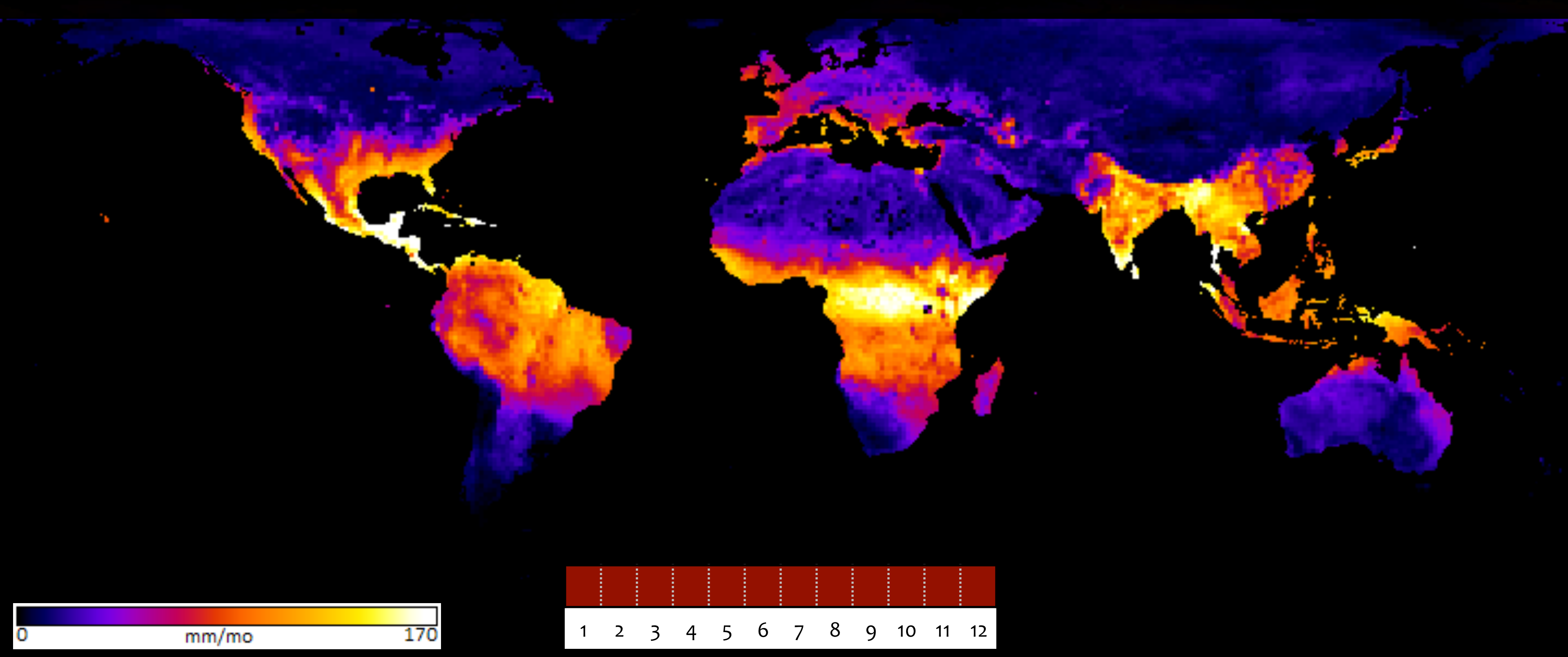

MONTHLY, 0.5 DEGREE

PT-JPL GLOBAL ET

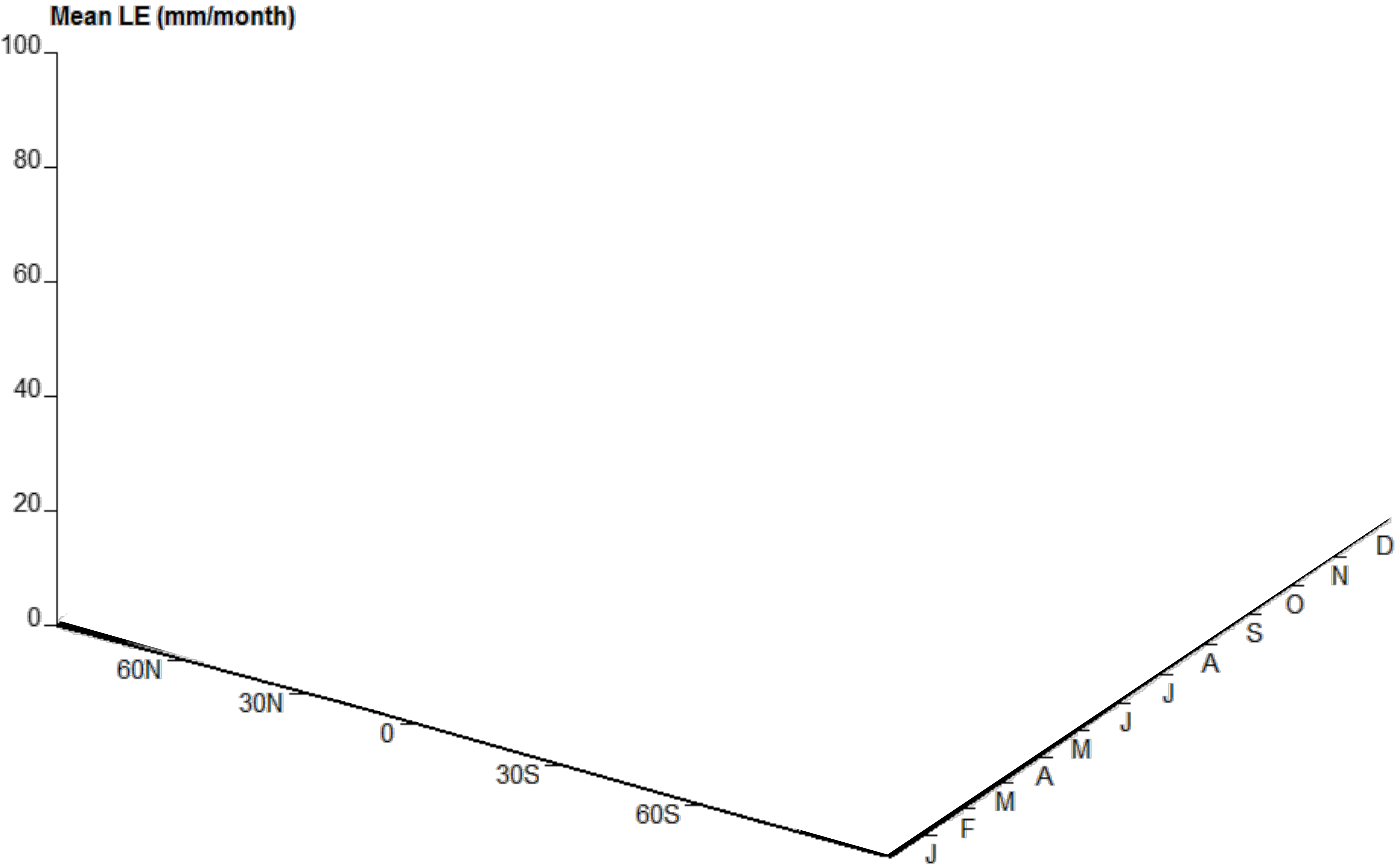

PT-JPL GLOBAL ET

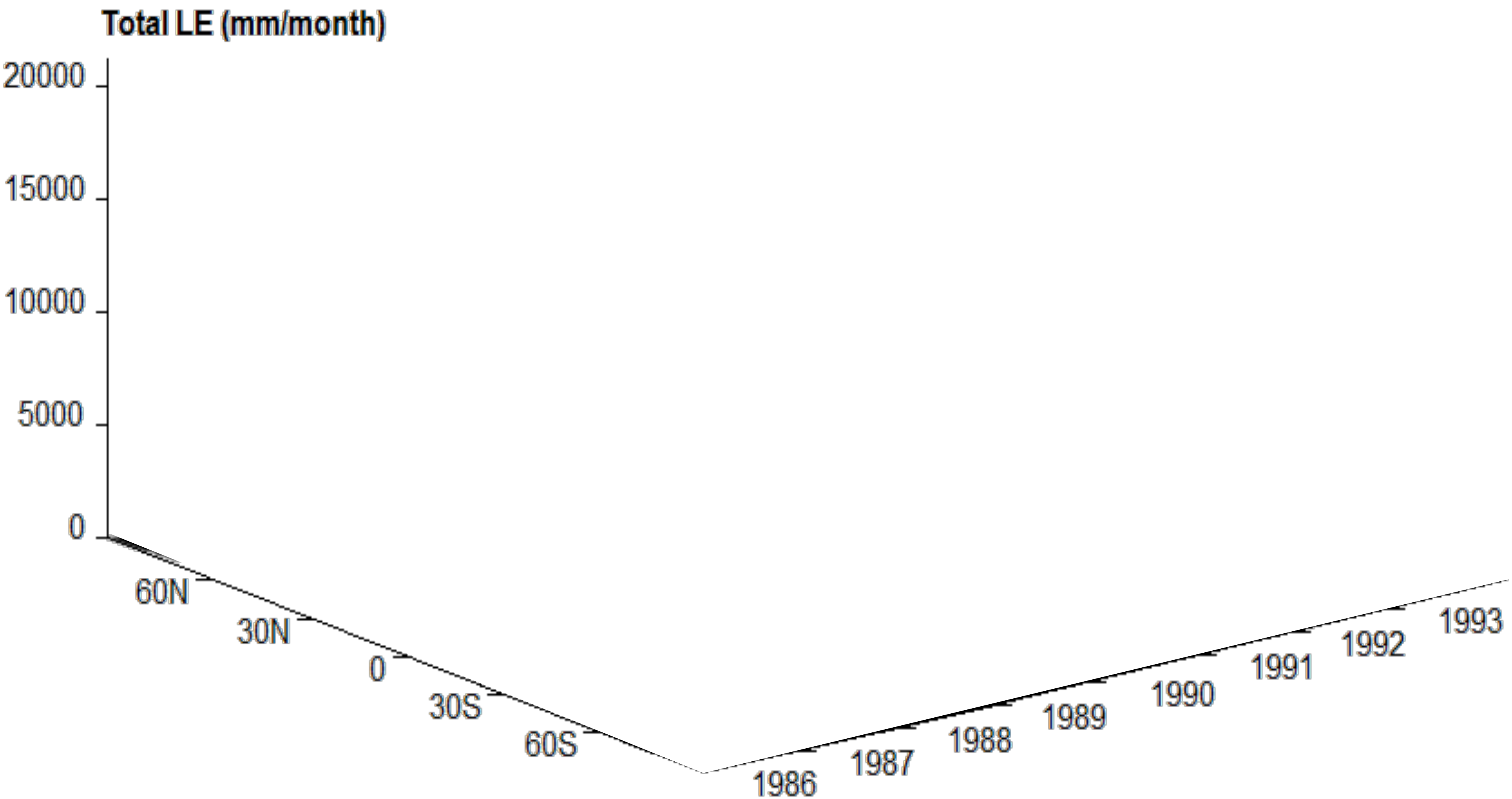

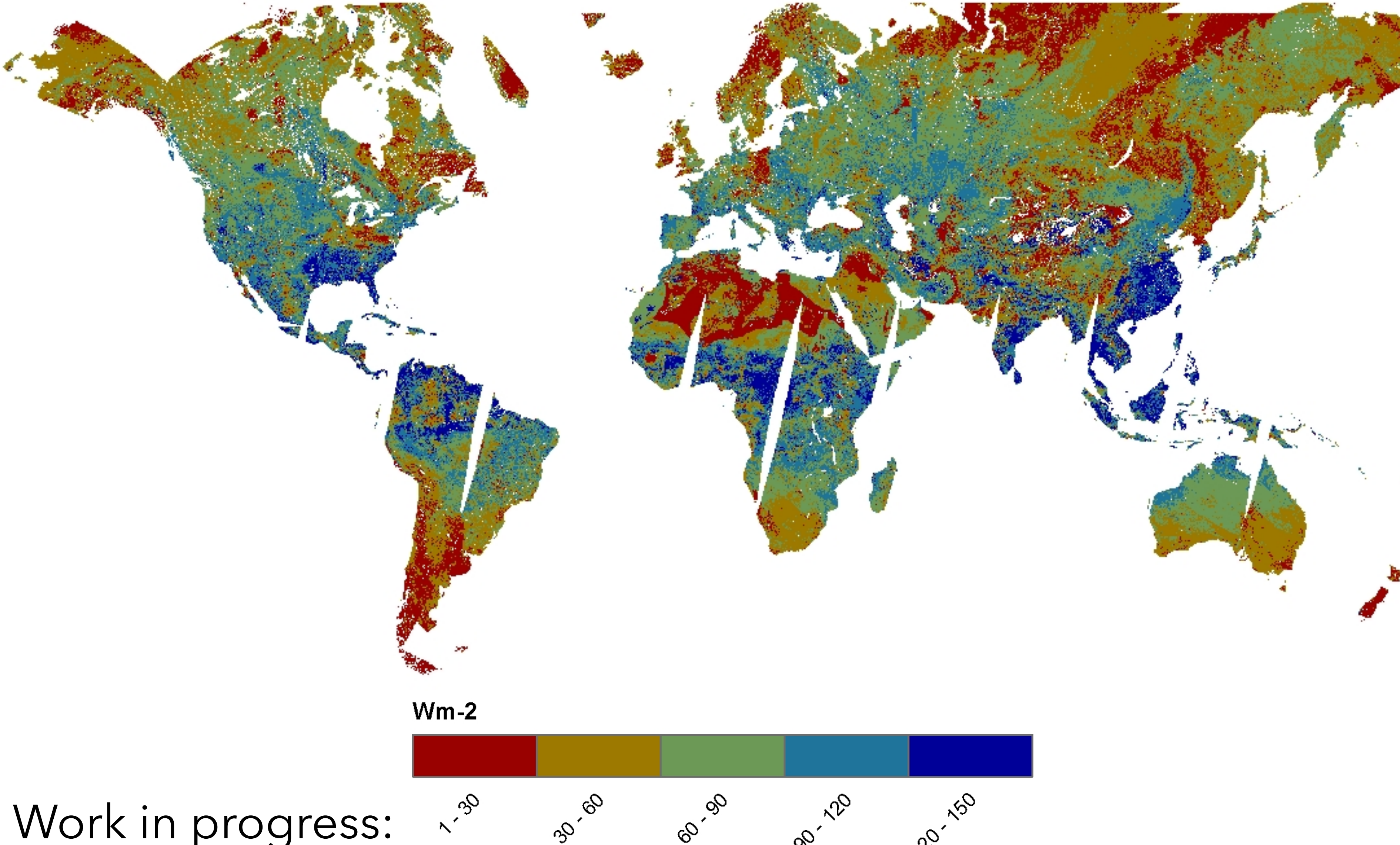

Work in progress:

- Global, 1 km, daily, MODIS-era (10+ years)
- PT-JPL, PM-MOD16, SEBS, PMBL

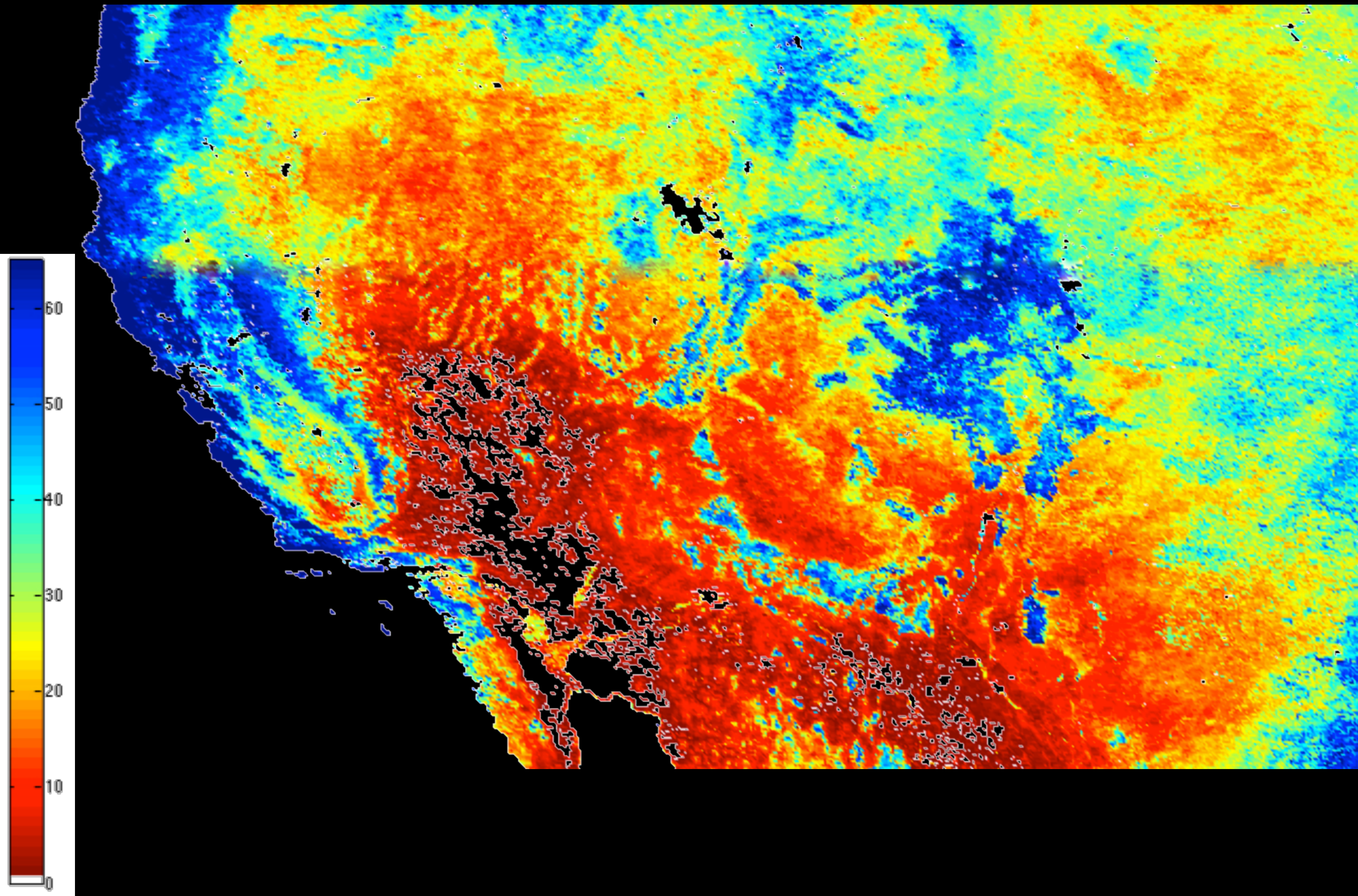
60
50
40
30
20
10
0

PT-JPL ET Landsat

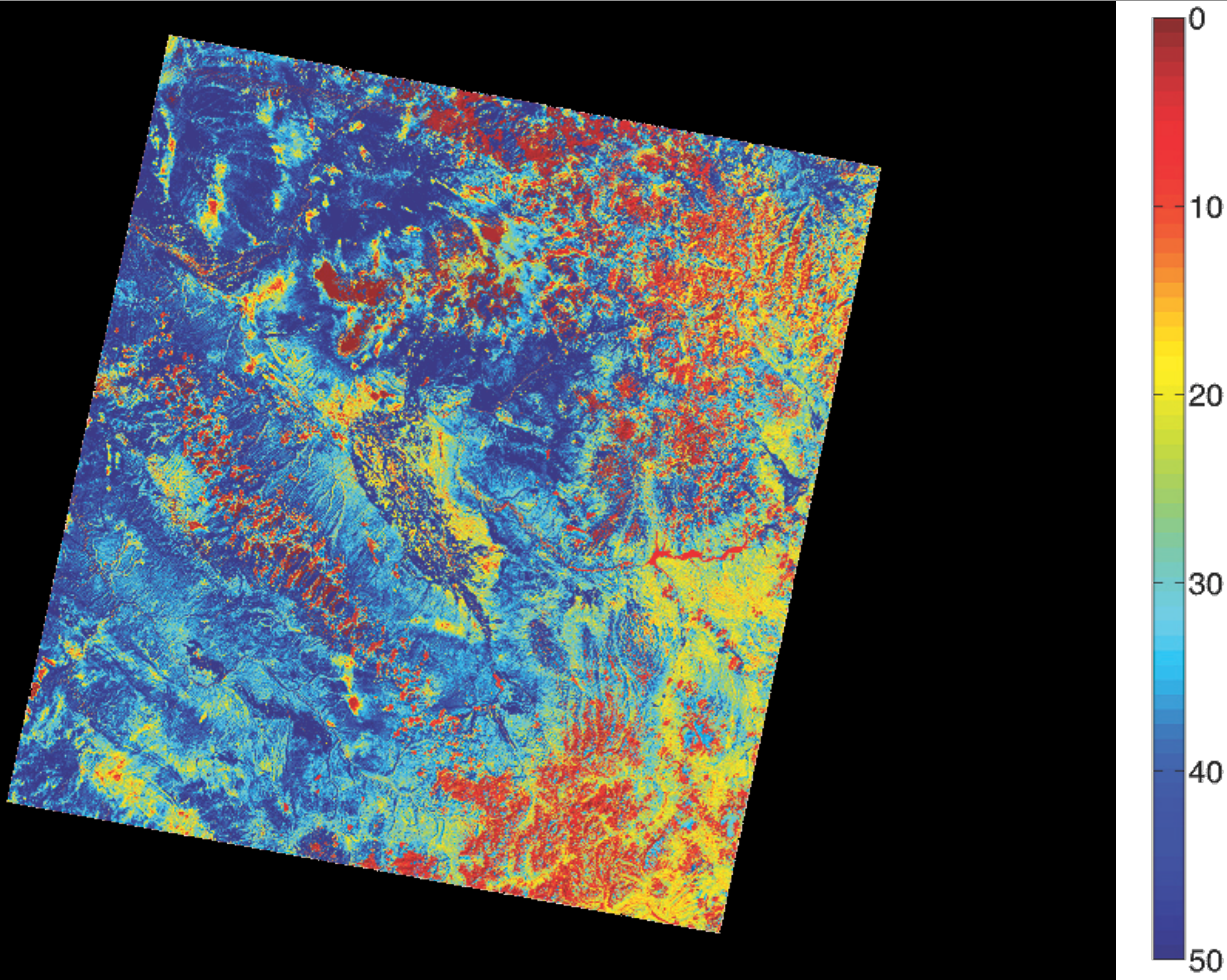

PT-JPL ET Landsat

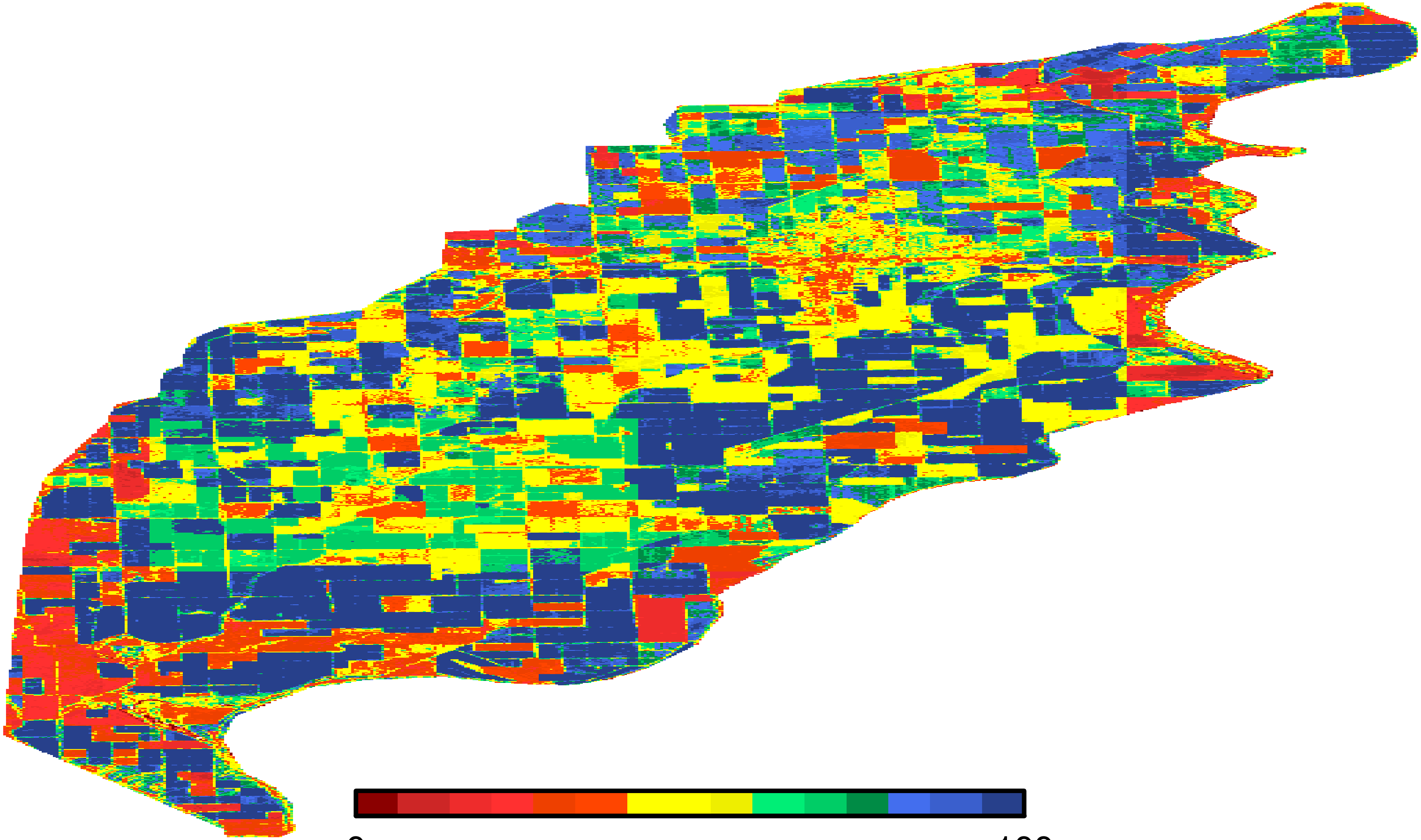

Remote Sensing of Environment 131 (2013) 103–118

Contents lists available at SciVerse ScienceDirect

Remote Sensing of Environment

journal homepage: www.elsevier.com/locate/rse

Actual evapotranspiration in drylands derived from in-situ and satellite data: Assessing biophysical constraints

Monica García [a,b,*], Inge Sandholt [a,b], Pietro Ceccato [b], Marc Ridler [a], Eric Mougin [c], Laurent Kergoat [c], Laura Morillas [d], Franck Timouk [c], Rasmus Fensholt [a], Francisco Domingo [d]

[a] Institute of Geography, University of Copenhagen, Øster Voldgade 10, DK-1350 Copenhagen, Denmark
[b] International Research Institute for Climate & Society, The Earth Institute, Columbia University, Lamont Campus, 61 Route 9W, Palisades, NY 10964-8000, USA
[c] Géosciences Environnement Toulouse (UMR 5563 UPS-CNRS-IRD) Observatoire Midi-Pyrénées (OMP), Université de Toulouse, 18 Avenue Edouard Belin 31401 Toulouse Cedex 9, France
[d] Desertification and Geoecology Dept. Estación Experimental de Zonas Áridas (EEZA), Consejo Superior de Investigaciones Científicas, Crtra. de Sacramento s/n La Cañada de San Urbano, E-04120 Almería, Spain

ARTICLE INFO

Article history:
Received 8 May 2012
Received in revised form 10 December 2012
Accepted 14 December 2012
Available online xxxx

Keywords:
Evapotranspiration
Surface temperature
Priestley–Taylor
Thermal inertia
MSG–SEVIRI
Water-limited ecosystems
MODIS

ABSTRACT

Improving regional estimates of actual evapotranspiration (λE) in water-limited regions located at climatic transition zones is critical. This study assesses an λE model (PT-JPL model) based on downscaling potential evapotranspiration according to multiple stresses at daily time-scale in two of these regions using MSG–SEVIRI (surface temperature and albedo) and MODIS products (*NDVI*, *LAI* and f_{PAR}). An open woody savanna in the Sahel (Mali) and a Mediterranean grassland (Spain) were selected as test sites with Eddy Covariance data used for evaluation. The PT-JPL model was modified to run at a daily time step and the outputs from eight algorithms differing in the input variables and also in the formulation of the biophysical constraints (stresses) were compared with the λE from the Eddy Covariance. Model outputs were also compared with other modeling studies at similar global dryland ecosystems.

The novelty of this paper is the computation of a key model parameter, the soil moisture constraint, relying on the concept of apparent thermal inertia ($f_{SM\text{-}ATI}$) computed with surface temperature and albedo observations. Our results showed that $f_{SM\text{-}ATI}$ from both in-situ and satellite data produced satisfactory results for λE at the Sahelian savanna, comparable to parameterizations using field-measured Soil Water Content (*SWC*) with r^2 greater than 0.80. In the Mediterranean grasslands however, with much lower daily λE values, model results were not as good as in the Sahel ($r^2 = 0.57$–0.31) but still better than reported values from more complex models applied at the site such as the Two Source Model (TSM) or the Penman–Monteith Leuning model (PML).

PT-JPL-daily model with a soil moisture constraint based on apparent thermal inertia, $f_{SM\text{-}ATI}$ offers great potential for regionalization as no field-calibrations are required and water vapor deficit estimates, required in the original

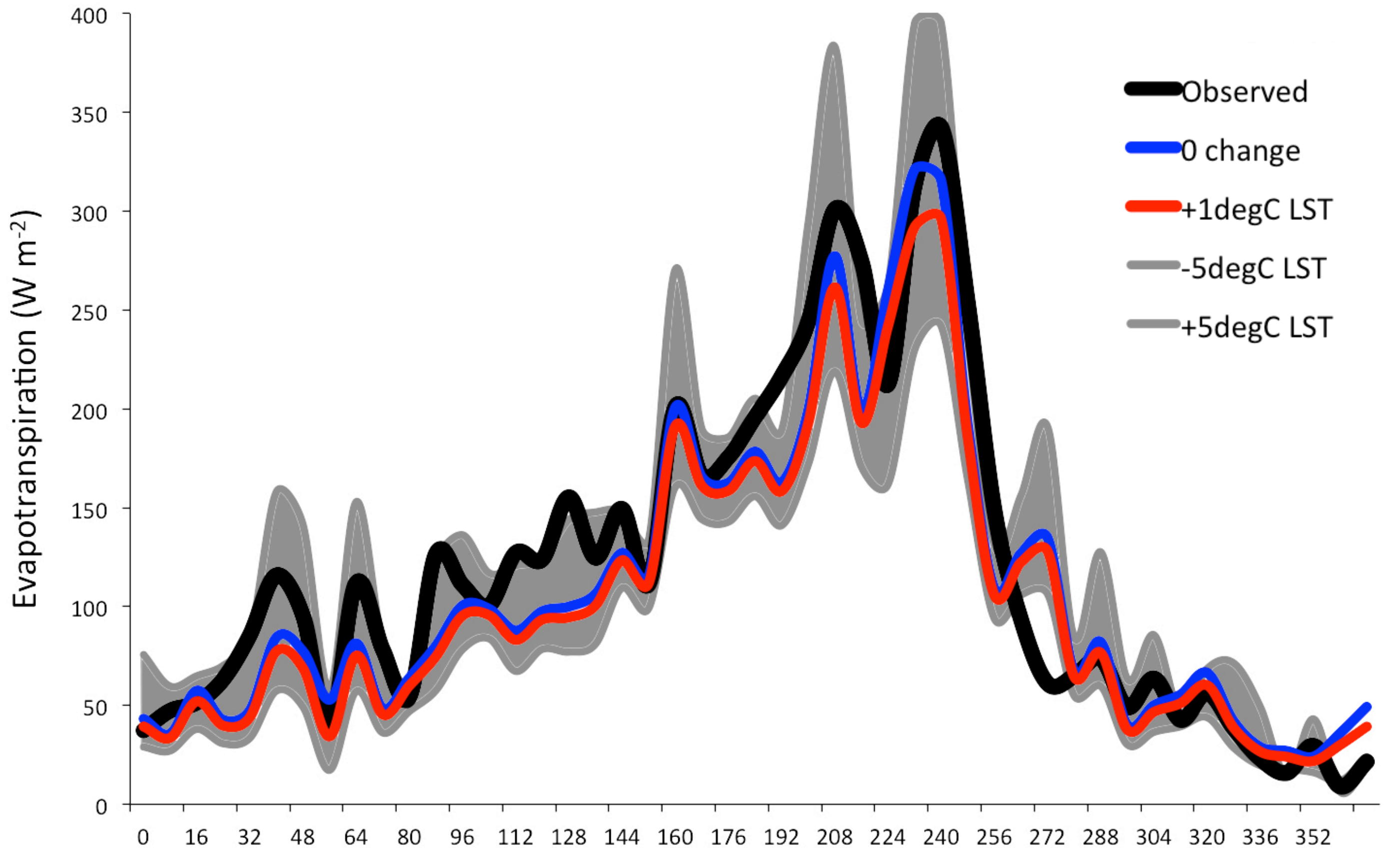

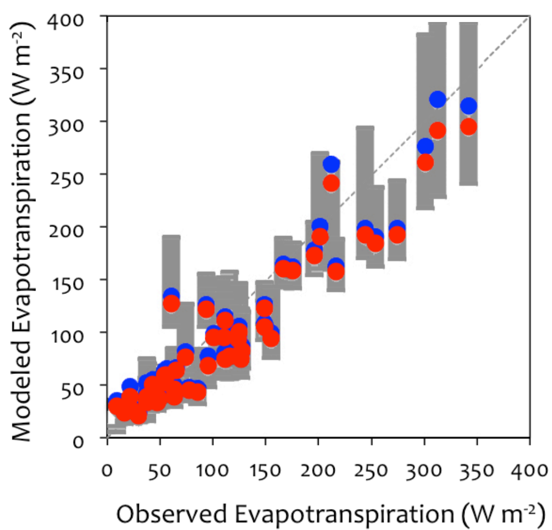

	0Δ	+1°C	±5°C
m			
r^2			
RMSE			

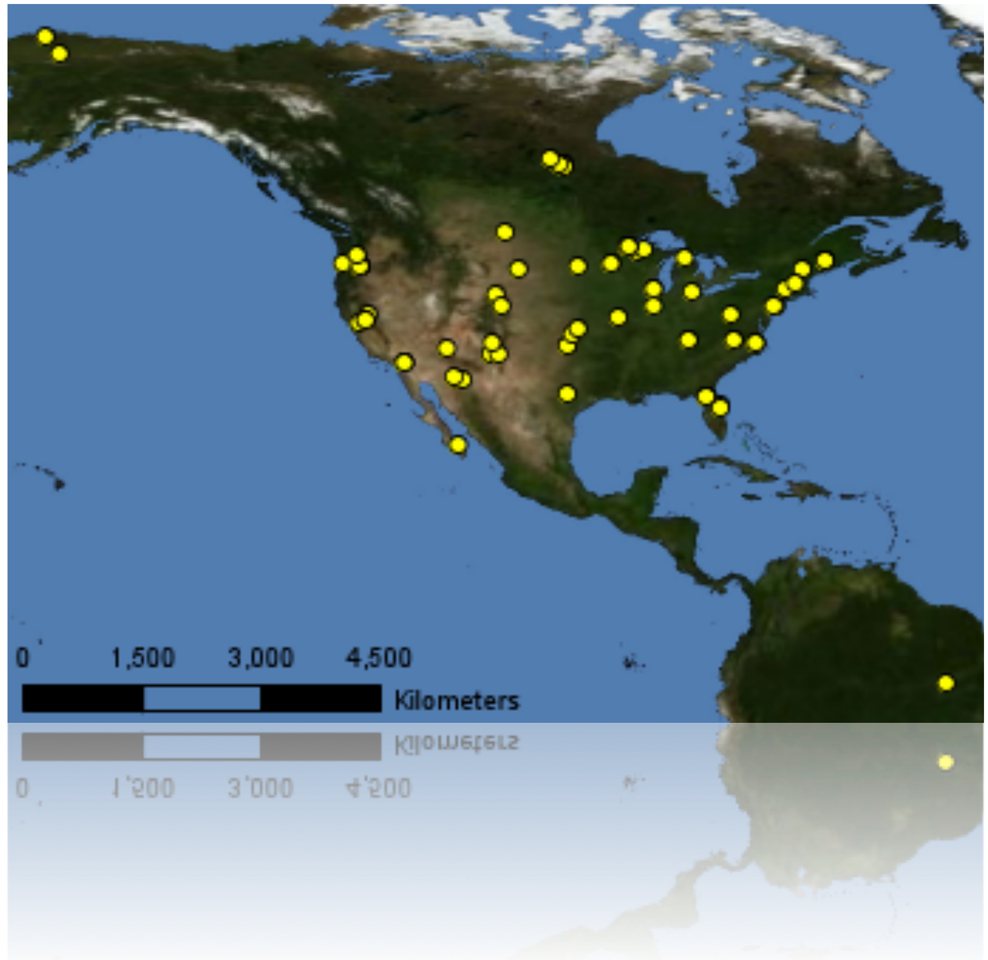
0
1,500
3,000
4,500
Kilometers

site-level ET uncertainty from LST uncertainty

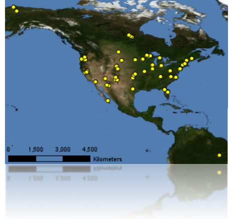

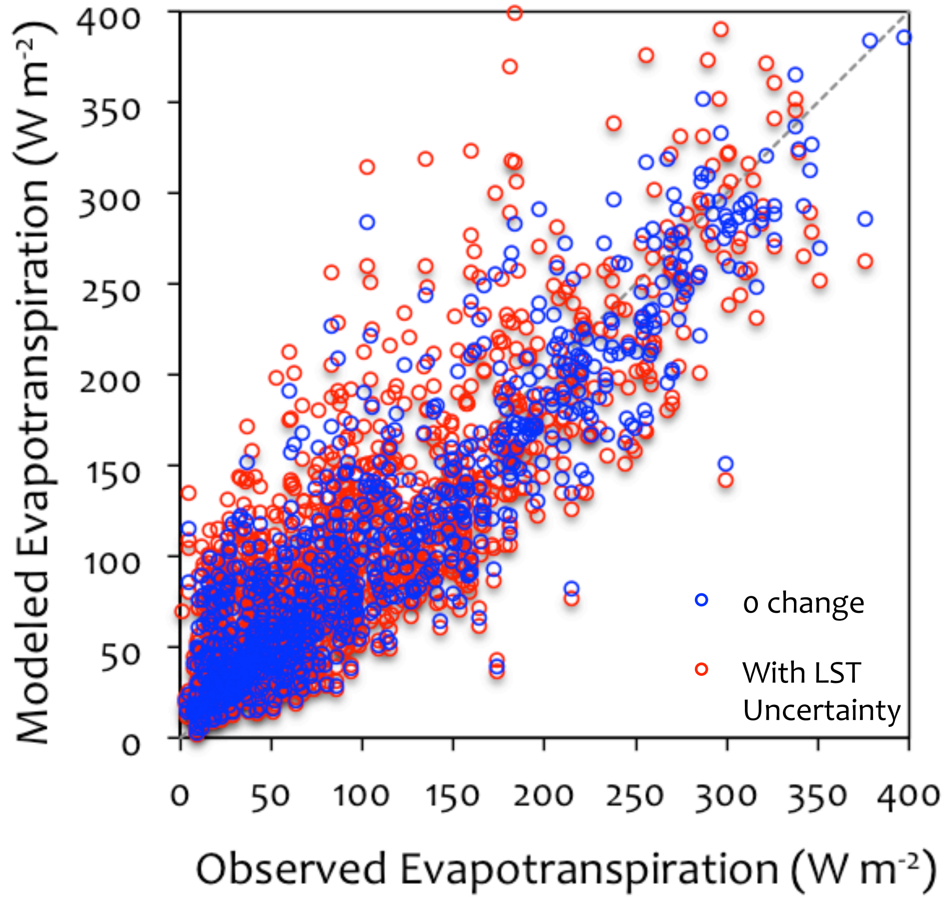

	0Δ	Δ◦C
m	0.99	
r^2	0.82	
RMSE	37.7	

site-level ET uncertainty sensitivity from LST uncertainty

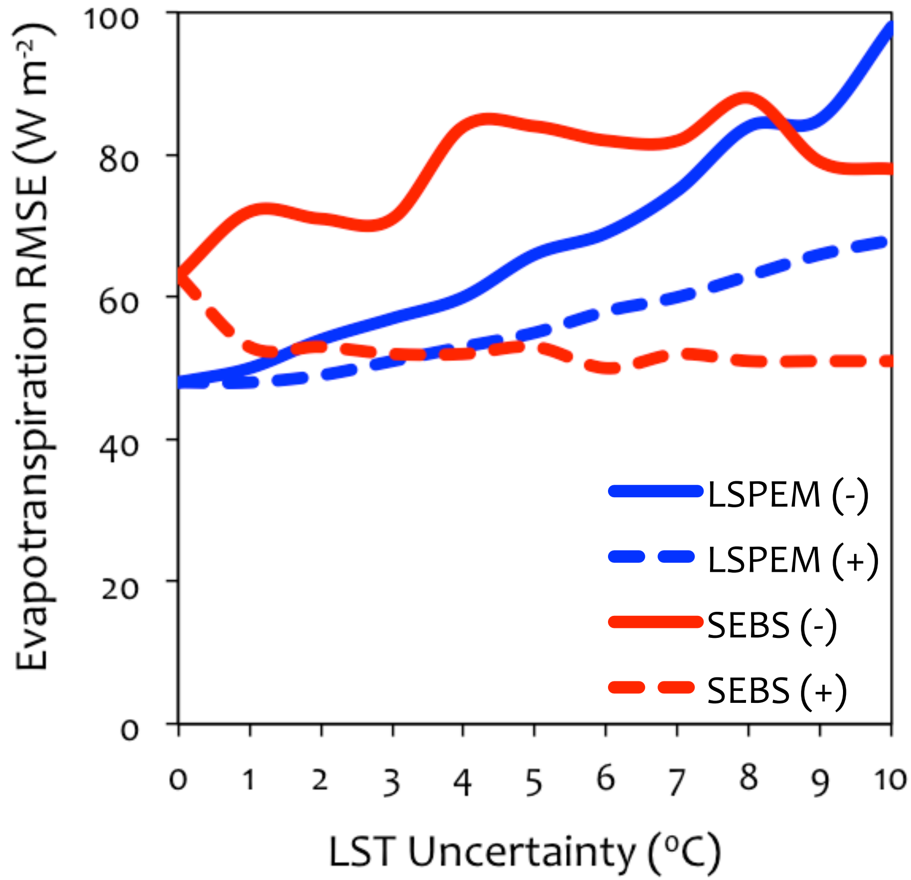

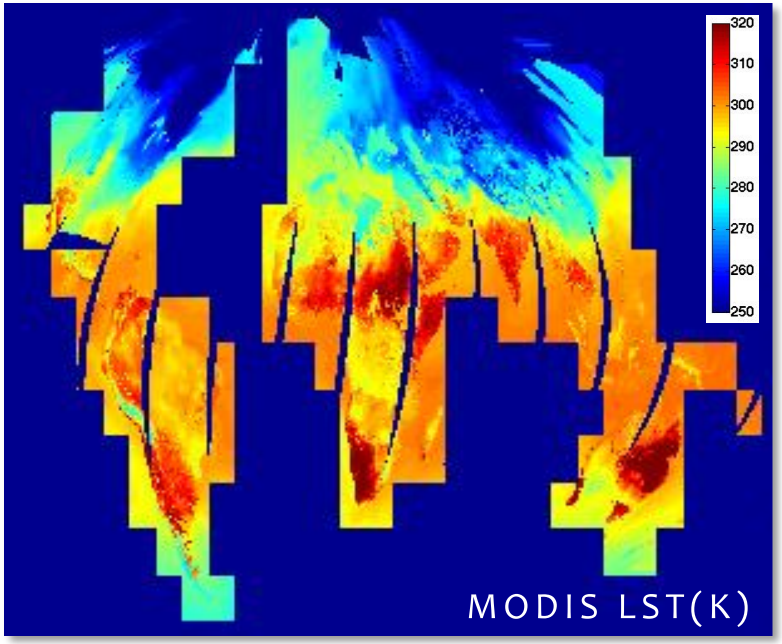

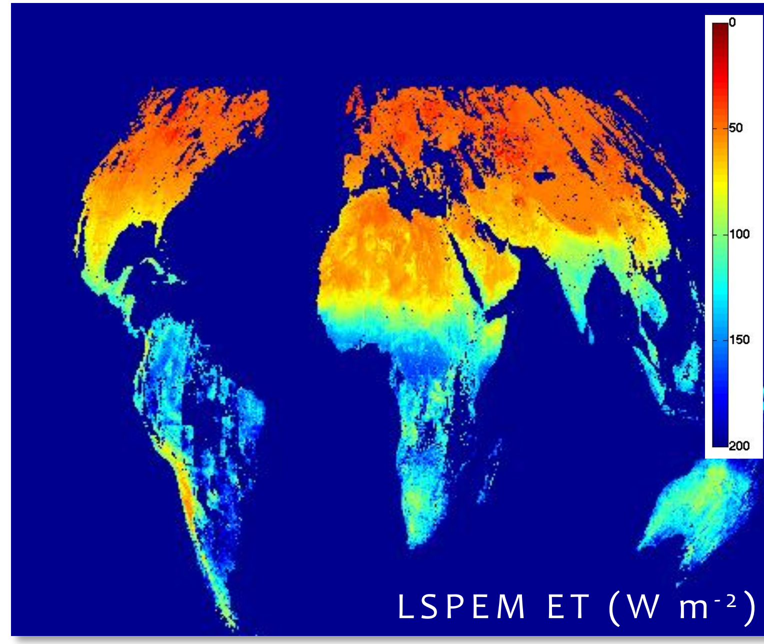

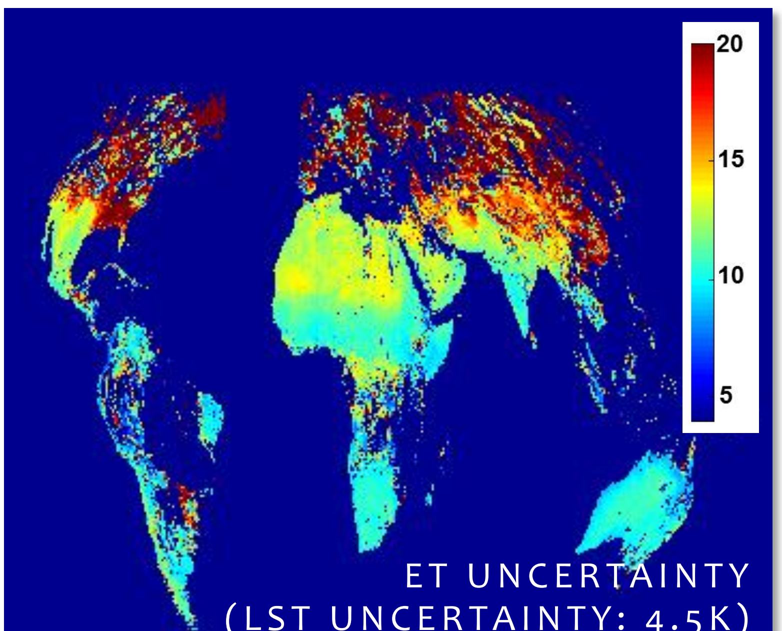

- **ET UNCERTAINTY**
  $= abs(ET^{LST0}-ET^{LST+})+abs(ET^{LST0}-ET^{LST-})$
  $= abs(50-51\ W\ m^{-2})+abs(50-58\ W\ m^{-2})$
  $= 9\ W\ m^{-2}$ (global mean)

- **ET SENSITIVITY**
  $= abs(ET^{LST+}-ET^{LST-})/ET^{LST0}$
  $= abs(51-58\ W\ m^{-2})/50\ W\ m^{-2}$
  = 14% (global mean)

AMAZON DROUGHT 2005

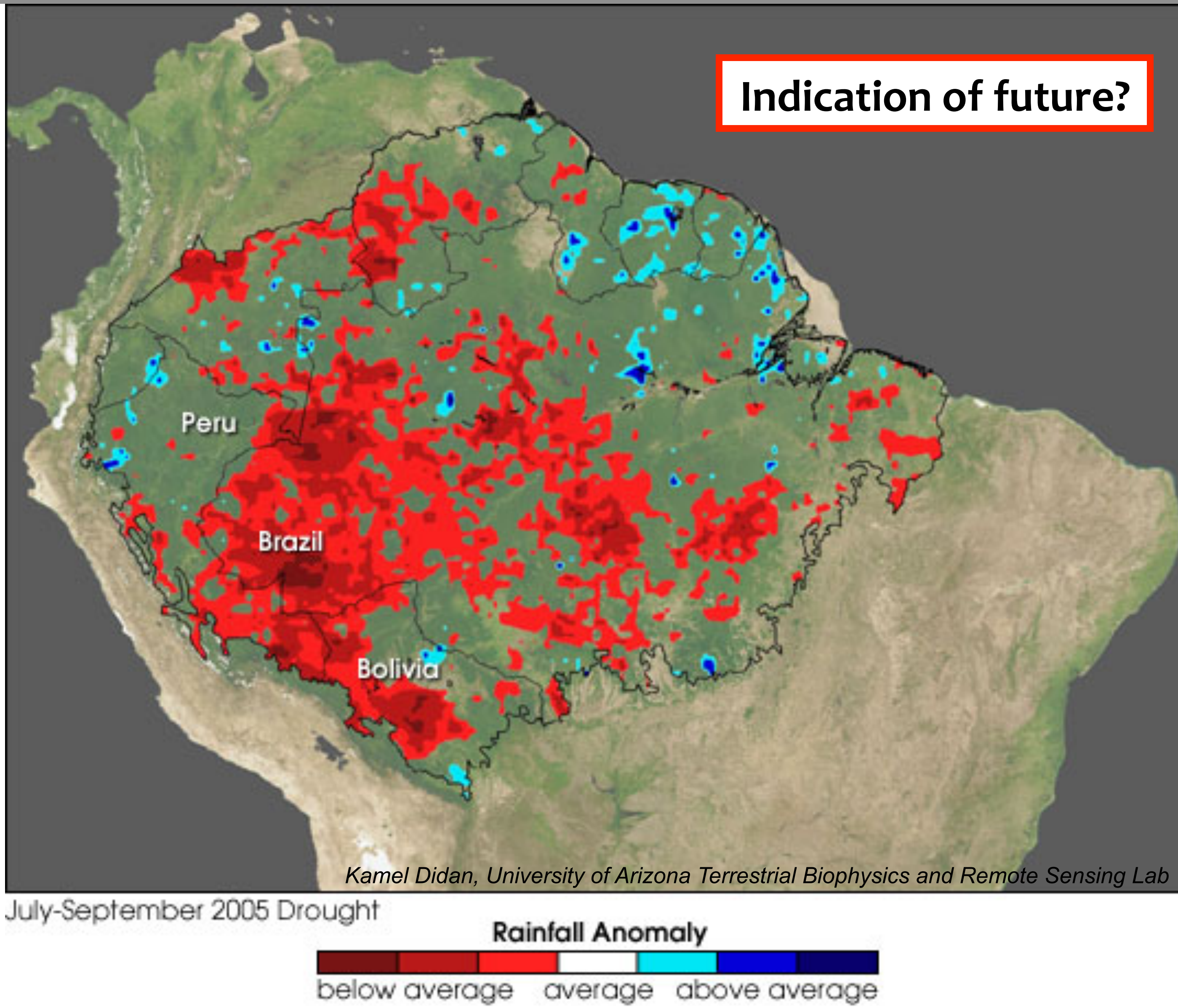

DROUGHT?

Drought: meteorological (or, climatological, atmospheric), agricultural, hydrologic, socio-economic; exceedance of threshold.

Vegetation drought: physical drying of soil such that the overlying vegetation experiences physiological water stress manifested in a reduction of productivity, loss of leaves/needles, and, ultimately, mortality.

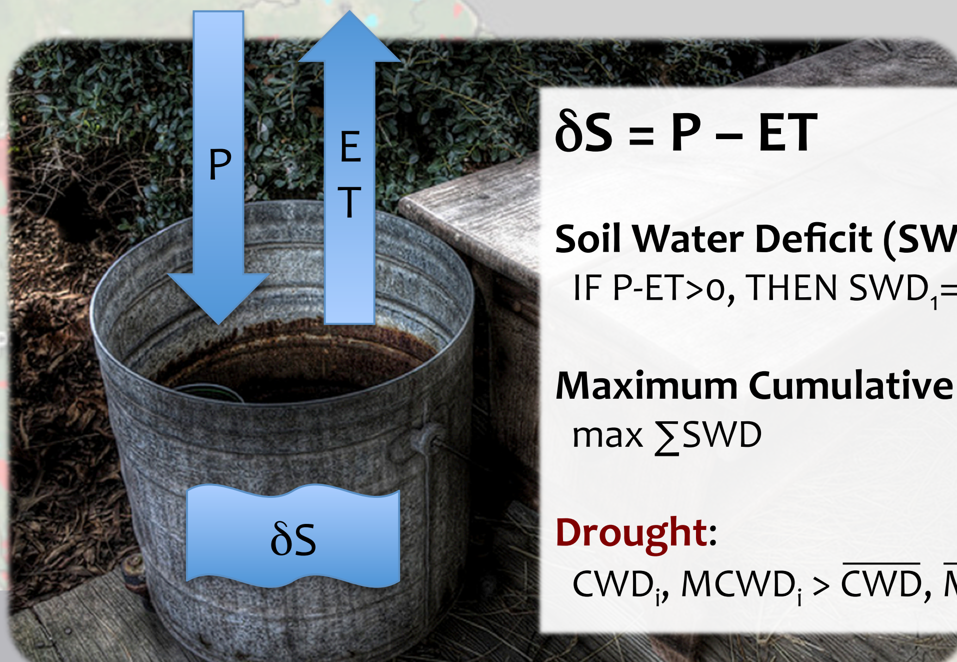

$\delta S = P - ET$

Soil Water Deficit (SWD):

IF P-ET>0, THEN $SWD_1=0$, ELSE $SWD_1=P-ET+SWD_0$

Maximum Cumulative Water Deficit (MCWD):

max $\sum SWD$

Drought:

$CWD_i, MCWD_i > \overline{CWD}, \overline{MCWD}$

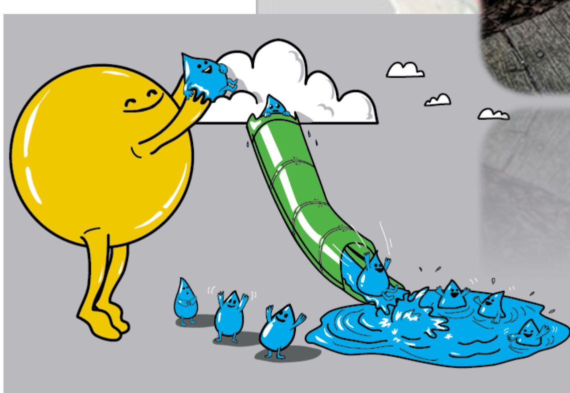

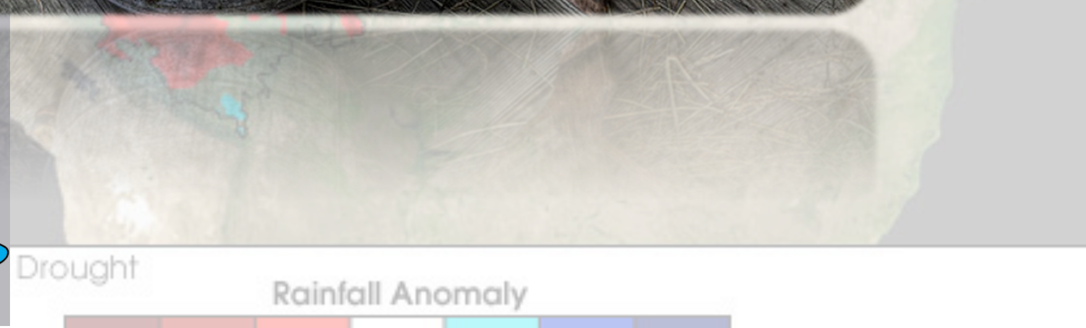

Fisher, J.B., Andreadis, K.M., 2013. Transpiration, physical evaporation and droughts. *Encyclopedia of Natural Resources*.

PRECIPITATION

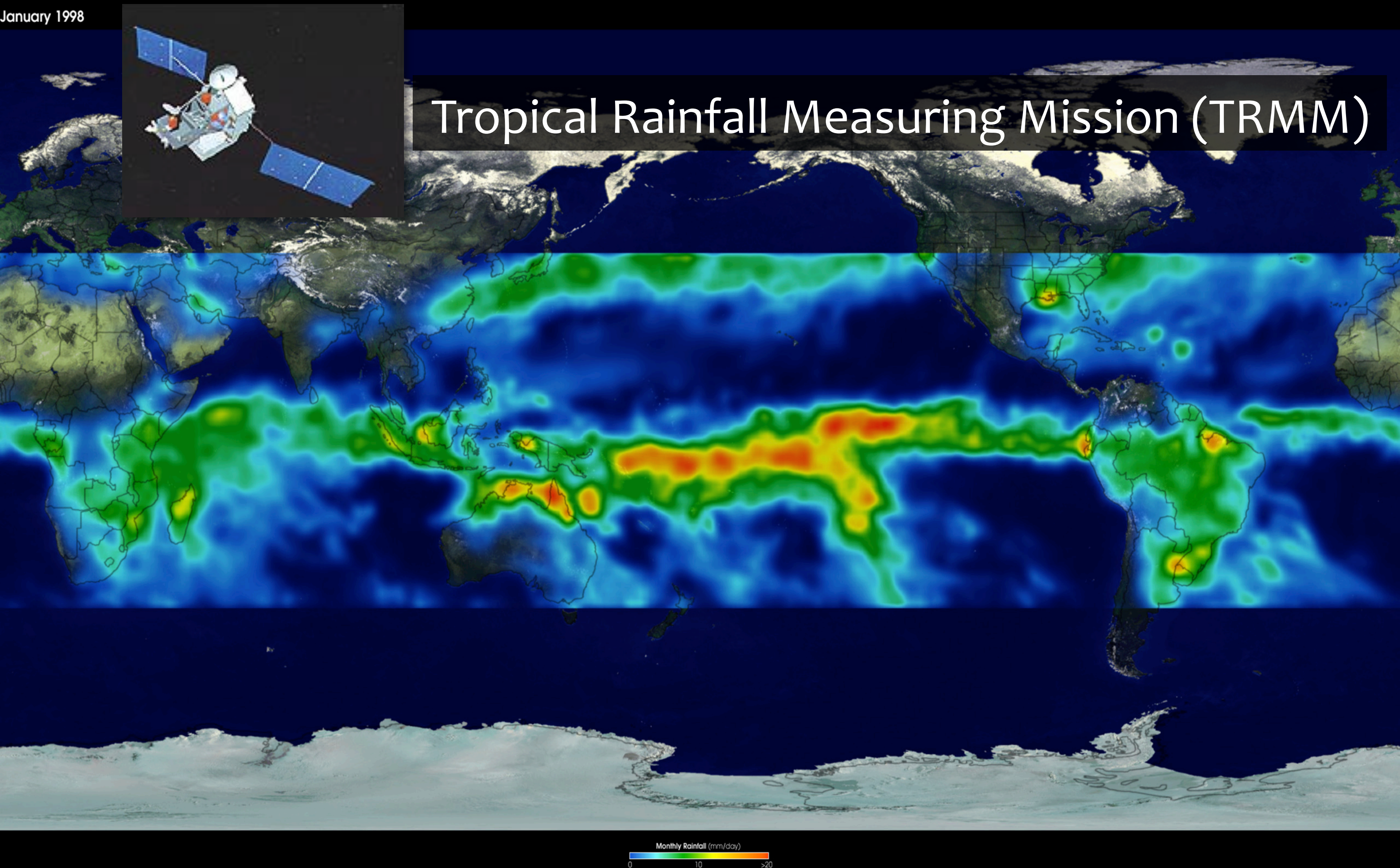

DROUGHT?

Drought: meteorological (or, climatological, atmospheric), agricultural, hydrologic, socio-economic; exceedance of threshold.

Vegetation drought: physical drying of soil such that the overlying vegetation experiences physiological water stress manifested in a reduction of productivity, loss of leaves/needles, and, ultimately, mortality.

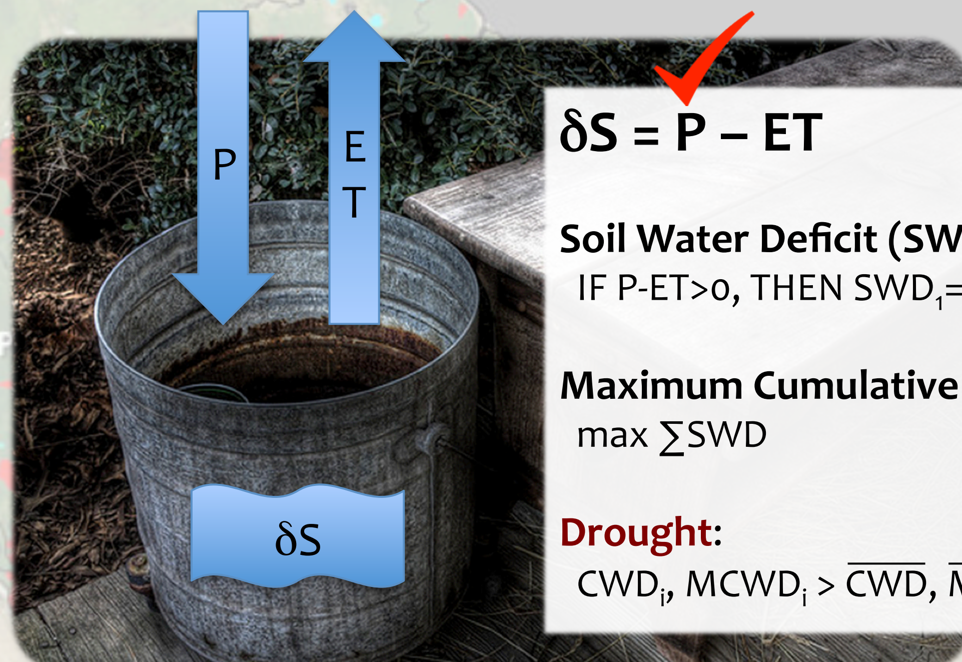

$$\delta S = P - ET$$

Soil Water Deficit (SWD):

IF P-ET>0, THEN $SWD_1=0$, ELSE $SWD_1=P-ET+SWD_0$

Maximum Cumulative Water Deficit (MCWD):

max $\sum SWD$

Drought:

CWD_i, $MCWD_i > \overline{CWD}$, $\overline{MCWD}$

July-September 2005 Drought

Rainfall Anomaly

Fisher, J.B., Andreadis, K.M., in press. Transpiration, physical evaporation and droughts. *Encyclopedia of Natural Resources*.

EVAPOTRANSPIRATION

Manaus

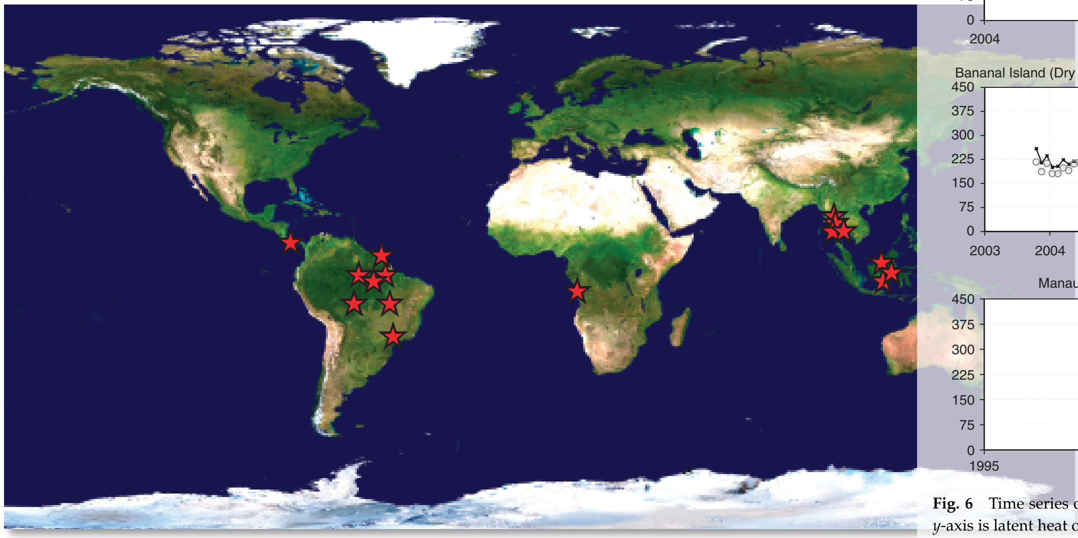

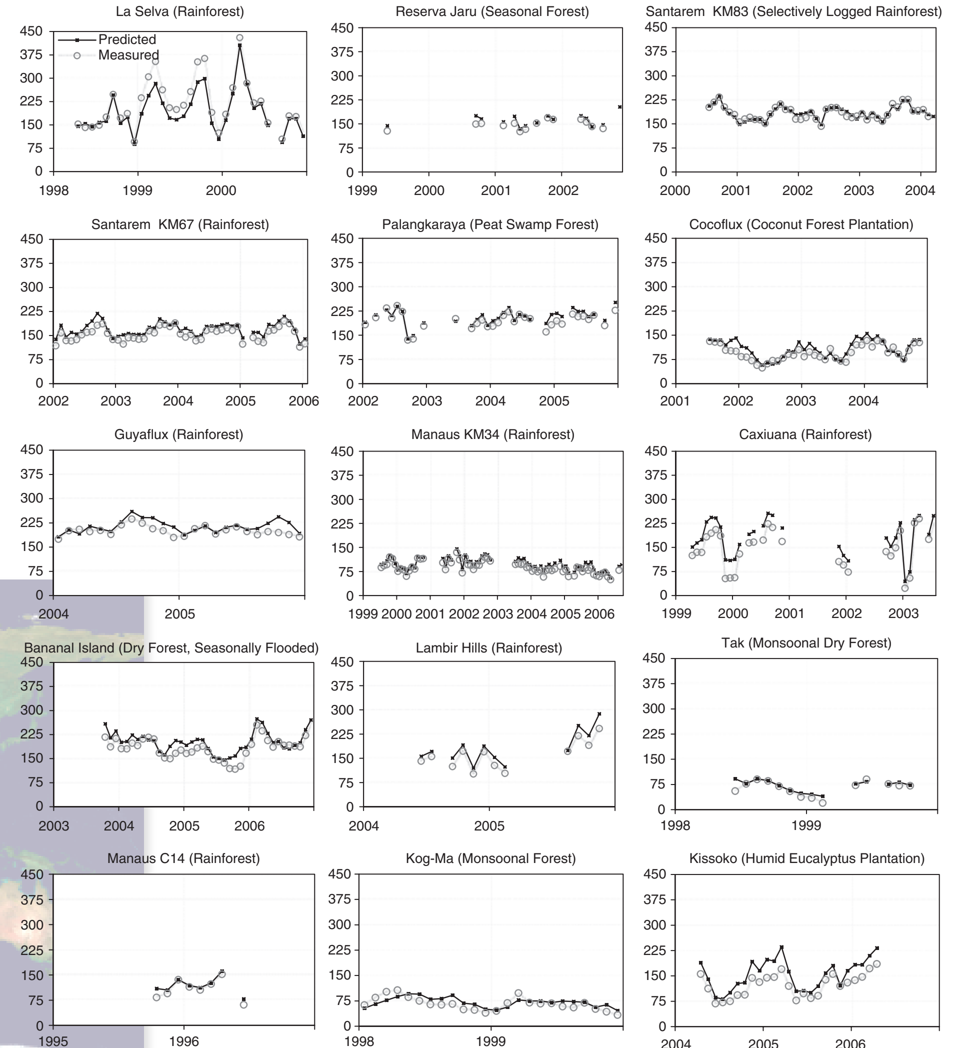

Fig. 6 Time series of tower measurements and model predictions at each site sorted in descending order by evaporative fraction. The *y*-axis is latent heat of evaporation (LE) (W m^{-2}) and *x*-axis is year. Open circles are observed and closed squares are predicted LE based on the FC model.

Fisher, J.B., et al., 2009. The land–atmosphere water flux in the tropics. *Global Change Biology*.

EVAPOTRANSPIRATION

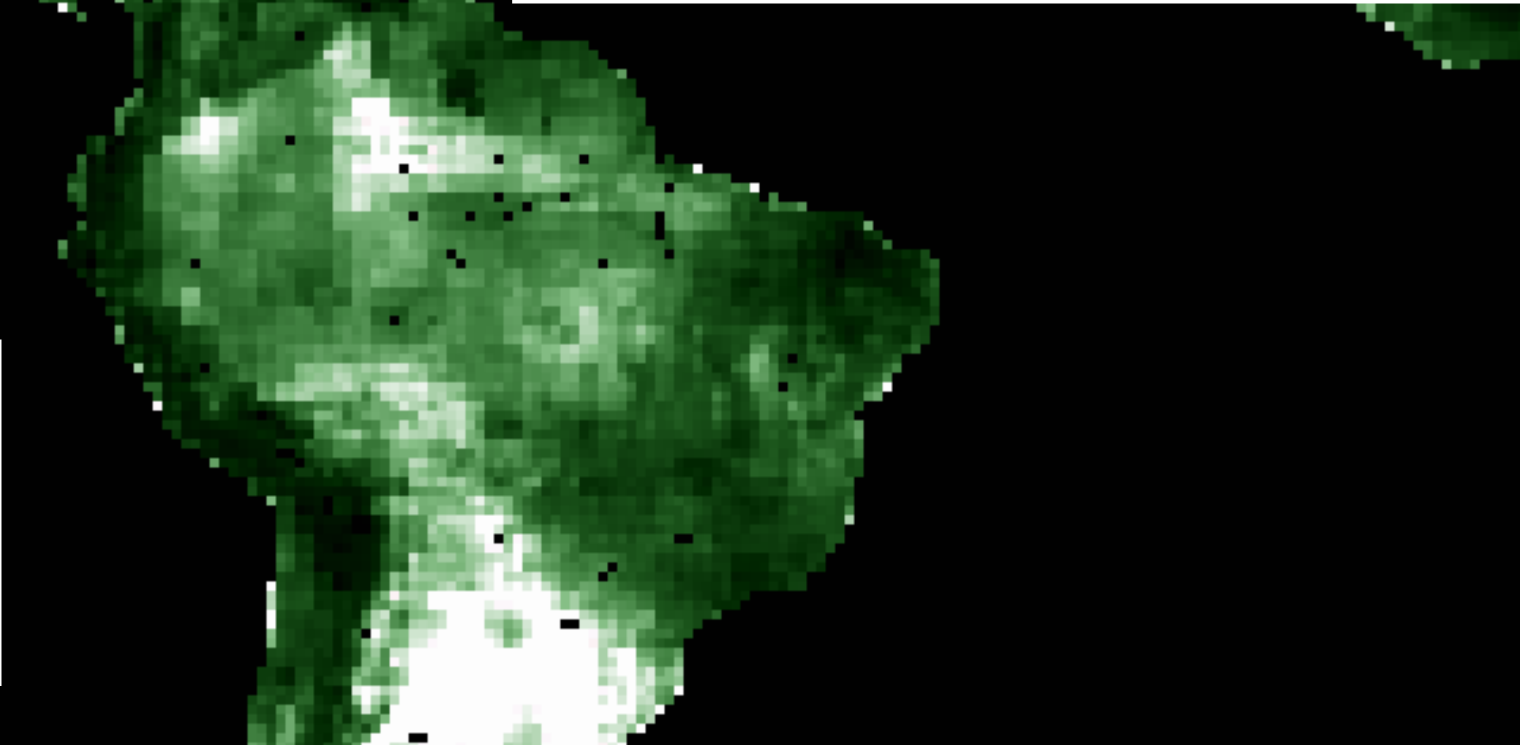

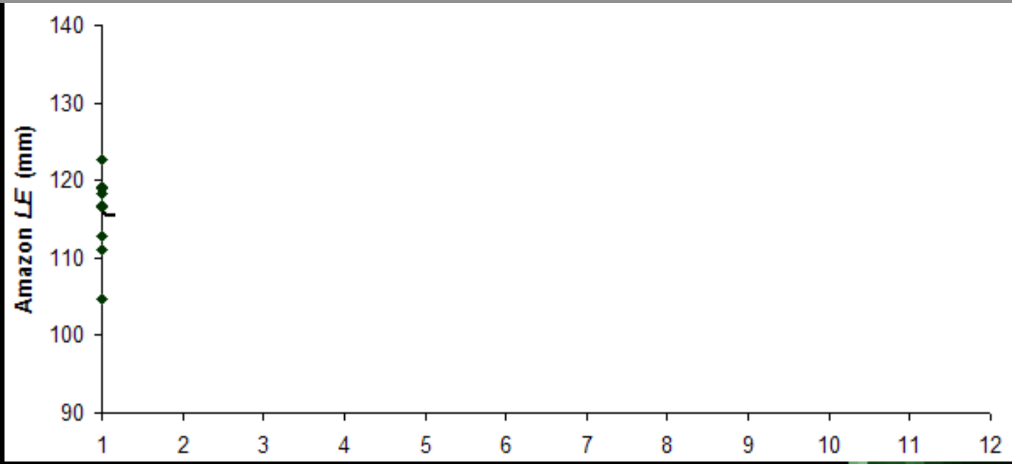

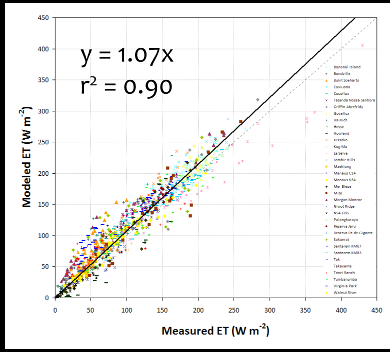

DROUGHT?

Drought: meteorological (or, climatological, atmospheric), agricultural, hydrologic, socio-economic; exceedance of threshold.

Vegetation drought: physical drying of soil such that the overlying vegetation experiences physiological water stress manifested in a reduction of productivity, loss of leaves/needles, and, ultimately, mortality.

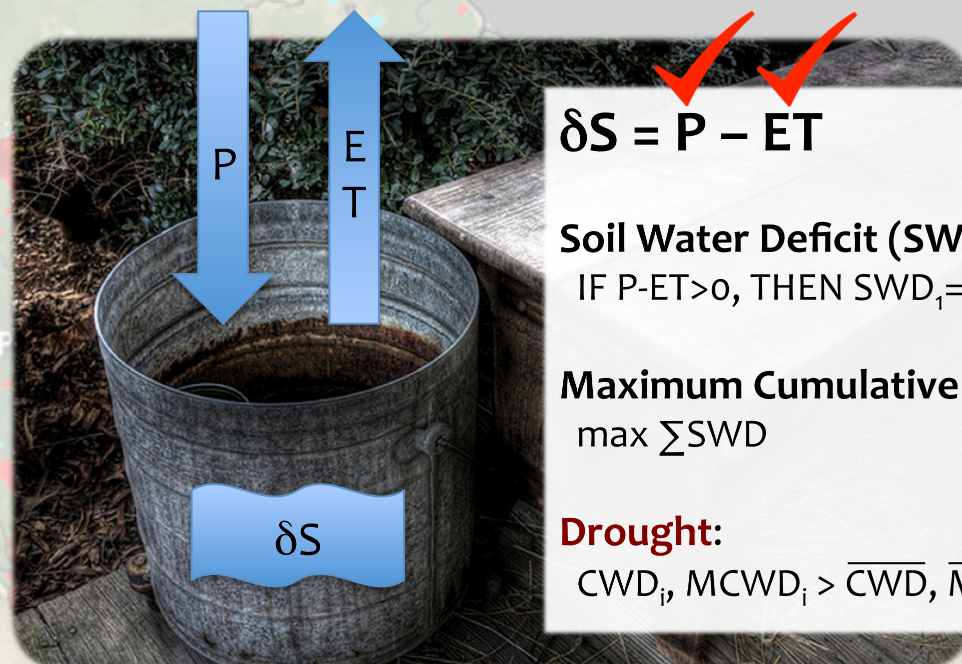

$$\delta S = P - ET$$

Soil Water Deficit (SWD):

IF P-ET>0, THEN $SWD_1=0$, ELSE $SWD_1=P-ET+SWD_0$

Maximum Cumulative Water Deficit (MCWD):

max $\sum SWD$

Drought:

CWD_i, $MCWD_i > \overline{CWD}$, $\overline{MCWD}$

July-September 2005 Drought

Rainfall Anomaly

Fisher, J.B., Andreadis, K.M., in press. Transpiration, physical evaporation and droughts. *Encyclopedia of Natural Resources*.

DROUGHT?

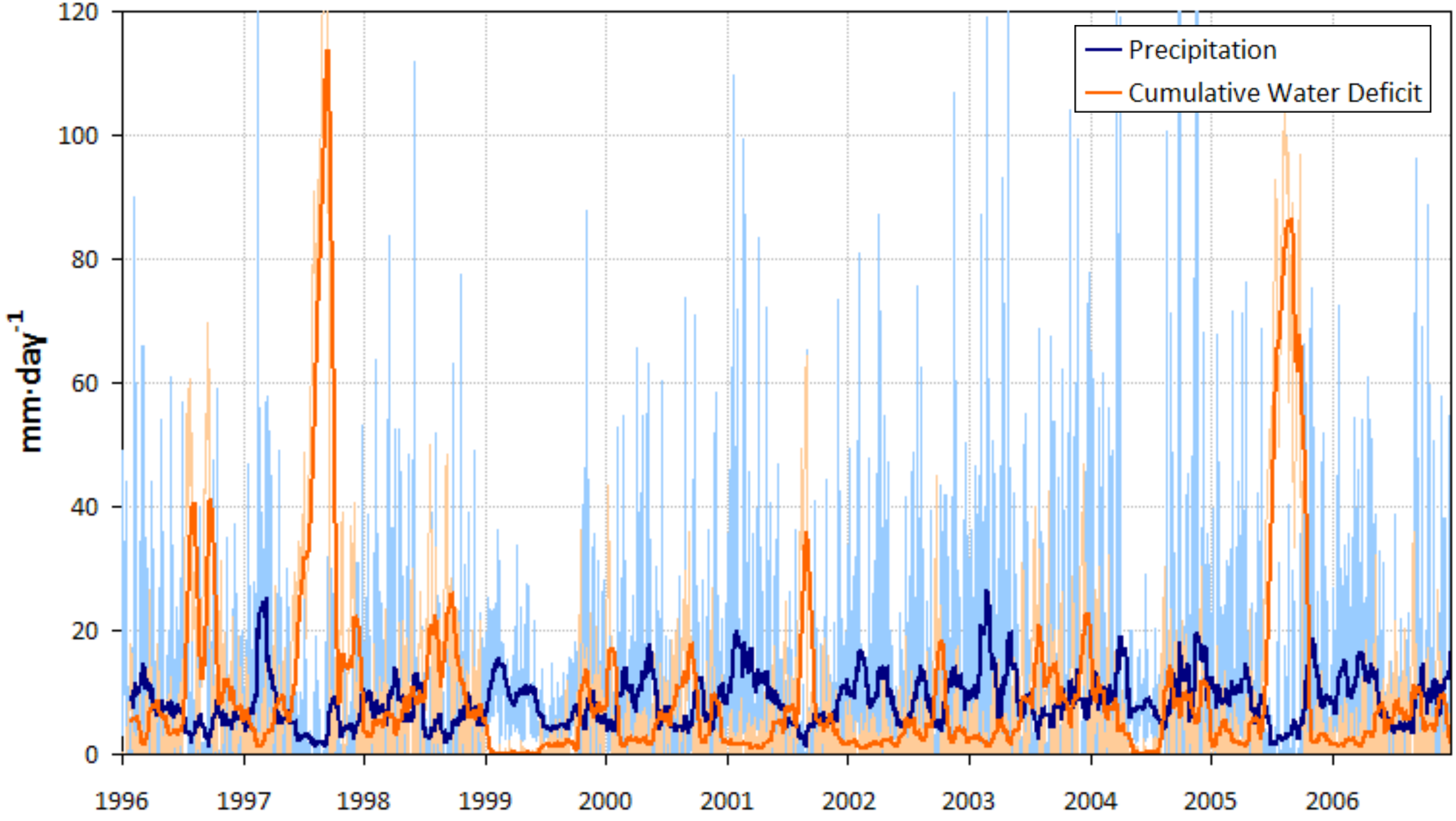

Phillips, O.L., Aragão, L., Lewis, S.L., **Fisher, J.B.**, et al., 2009. Drought sensitivity of the Amazon rainforest. *Science*.

MORTALITY?

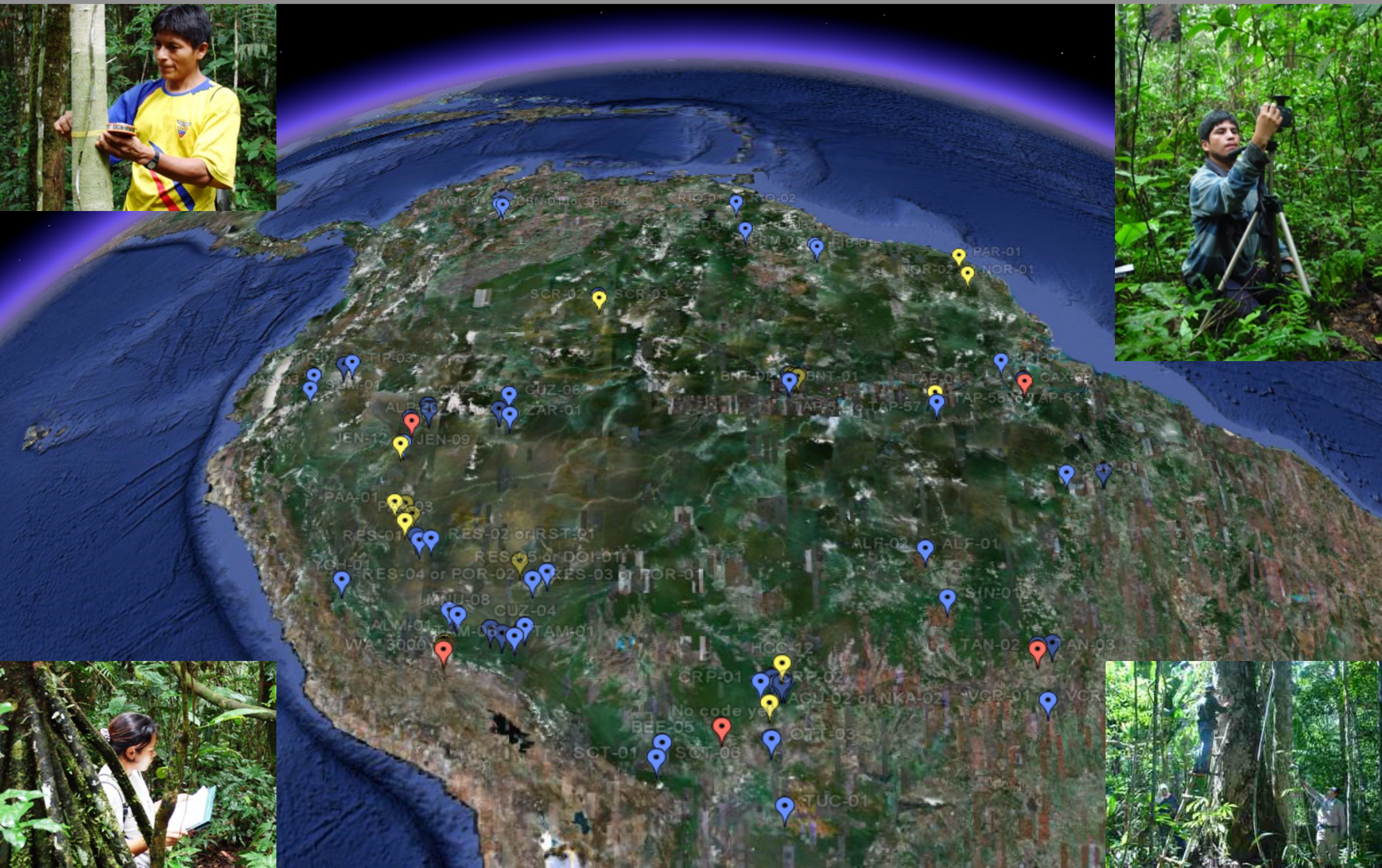

PAR-01
NOR-01
SCR-02
SCR-03
BNT-02
BNT-01
TIP-03
CUZ-05
CUZ-06
ZAR-01
JEN-12
JEN-09
PAA-01
RES-01
RES-02 or RST-01
RES-05 or DOI-01
RES-04 or POR-02
RES-03 or POR-01
YCH-01
MNU-08
CUZ-04
TAM-01
WA_3000
TAP-57
CAX-06
ALF-02
ALF-01
SIN-01
TAN-02
TAN-03
HCC-12
CRP-01
CRP-02
ACU-02 or NKA-02
VCR-01
BEE-05
SCT-01
SCT-06
OTT-03
TUC-01

As drought increases, live trees decrease.

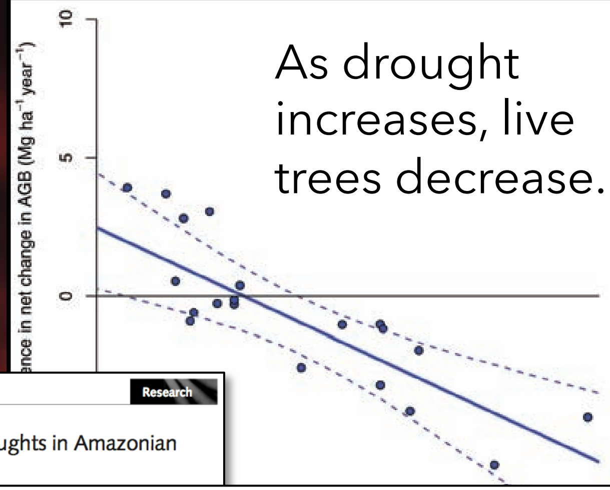

Exploring the likelihood and mechanism of a climate-change-induced dieback of the Amazon rainforest

Yadvinder Malhi, Luiz E. O. C. Aragão, David Galbraith, Chris Huntingford, Rosie Fisher, Przemyslaw Zelazowski, Stephen Sitch, Carol McSweeney, and Patrick Meir

Seasonal and interannual variability of climate and vegetation indices across the Amazon

Paulo M. Brando, Scott J. Goetz, Alessandro Baccini, Daniel C. Nepstad, Pieter S. A. Beck, and Mary C. Christman

Research review

Drought impacts on the Amazon forest: the remote sensing perspective

Gregory P. Asner

New Phytologist (2010) 187: 569–578
doi: 10.1111/j.1469-8137.2010.03310.x

Remote sensing detection of droughts in Amazonian forest canopies

Liana O. Anderson, Yadvinder Malhi, Luiz E. O. C. Aragão, ... and Oliver Phillips

New Phytologist (2010) 187: 733–750
doi: 10.1111/j.1469-8137.2010.03355.x

GEOPHYSICAL RESEARCH LETTERS, VOL. 38, L07402, doi:10.1029/2011GL046824, 2011

Widespread decline in greenness of Amazonian vegetation due to the 2010 drought

Liang Xu, Arindam Samanta, Marcos H. Costa, Ramakrishna R. Nemani, and Ranga B. Myneni

GEOPHYSICAL RESEARCH LETTERS, VOL. 38, L19105, doi:10.1029/2011GL049118, 2011

Amazon vegetation greenness as measured by satellite sensors over the last decade

P. M. Atkinson, J. Dash, and C. Jeganathan

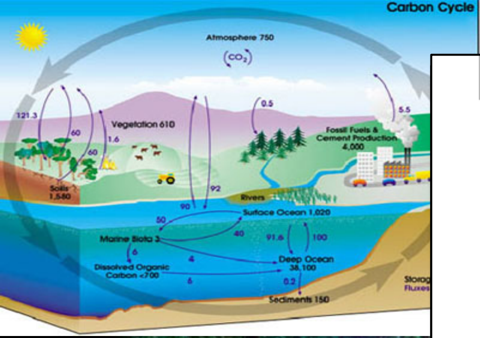

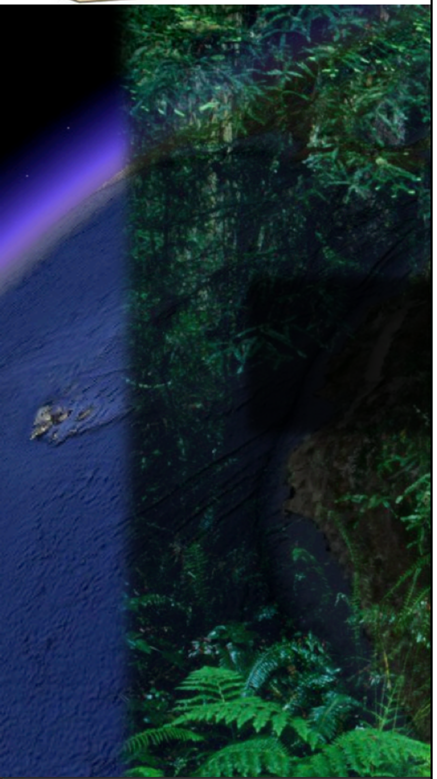

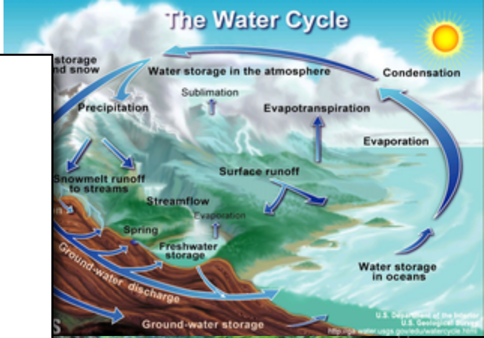

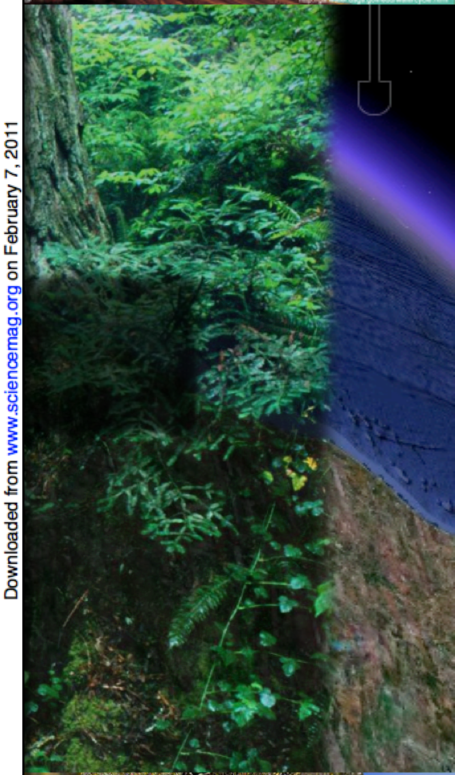

The 2010 Amazon Drought

Simon L. Lewis,[1]*† Paulo M. Brando,[2,3]* Oliver L. Phillips,[1] Geertje M. F. van der Heijden,[4] Daniel Nepstad[2]

Several global circulation models (GCMs) project an increase in the frequency and severity of drought events affecting the Amazon region as a consequence of anthropogenic greenhouse gas emissions (*1*). The proximate cause is twofold, increasing Pacific sea surface temperatures (SSTs), which may intensify El Niño Southern Oscillation events and associated periodic Amazon droughts, and an increase in the frequency of historically rarer droughts associated with high Atlantic SSTs and northwest displacement of the intertropical convergence zone (*1*, *2*). Such droughts may lead to a loss of some Amazon forests, which would accelerate climate change (*3*). In 2005, a major Atlantic SST–associated drought occurred, identified as a 1-in-100-year event (*2*). Here, we report on a second drought in 2010, when Atlantic SSTs were again high.

We calculated standardized anomalies from a decade of satellite-derived dry-season rainfall data (Tropical Rainfall Measuring Mission, 0.25° resolution) across 5.3 million km^2 of Amazonia for 2010 and 2005 (*4*). We used identical reference periods to allow a strict comparison of both drought events (*4*). On the basis of this index, the 2010 drought was more spatially extensive than the 2005 drought (rainfall anomalies ≤ −1 SD over 3.0 million km^2 and 1.9 million km^2 in 2010 and 2005, respectively; Fig. 1 and fig. S1). Because dry-season anomalies do not necessarily correlate with water stress for forest trees, we also calculated the maximum climatological water deficit (MCWD) for each year as the most negative cumulative value of water input minus estimated forest evapotranspiration (*5*). This measure of drought intensity correlates with Amazon forest tree mortality (*6*). In 2010, the difference in MCWD from the decadal mean that significantly increases tree mortality (≤ −25 mm) spanned 3.2 million km^2, compared with 2.5 million km^2 in 2005. The 2010 drought had three identifiable epicenters in southwestern Amazonia, north-central Bolivia, and Brazil's Mato Grosso state. In 2005 only a single southwestern Amazonia epicenter was detectable (fig. S1).

The relationship between the change in MCWD and changes in aboveground carbon storage derived from forest inventory plots affected by the 2005 drought (*6*) provides a first approximation of the biomass carbon impact of the 2010 event. Summing the change in carbon storage predicted by the 2010 MCWD difference across Amazonia gives a total impact of 2.2 Pg C [95% confidence intervals (CI) 1.2 and 3.4], compared with 1.6 Pg C for the 2005 event (CI 0.8, 2.6). These values are relative to the predrought carbon uptake and represent the sum of (*1*) the temporary cessation of biomass increases over the 2-year drought measurement interval (~0.8 Pg C) and (*2*) biomass lost via tree mortality, a committed carbon flux from decomposition over several years (~1.4 Pg C after the 2010 drought). In most years, these forests are a carbon sink; drought reverses this sink.

Considerable uncertainty remains, related to the soil characteristics within the epicenters of the 2010 drought, which could moderate or exacerbate climatic drying, whether a second drought will kill more trees (i.e., those damaged by the initial drought) or fewer (i.e., if most drought-susceptible trees are already dead), and whether drought slows soil respiration (temporarily offsetting the biomass carbon source). New field measurements will be required to refine our initial estimates.

The two recent Amazon droughts demonstrate a mechanism by which remaining intact tropical forests of South America can shift from buffering the increase in atmospheric carbon dioxide to accelerating it. Indeed, two major droughts in a decade may largely offset the net gains of ~0.4 Pg C $year^{-1}$ in intact Amazon forest aboveground biomass in nondrought years. Thus, repeated droughts may have important decadal-scale impacts on the global carbon cycle.

Droughts co-occur with peaks of fire activity (*5*). Such interactions among climatic changes, human actions, and forest responses represent potential positive feedbacks that could lead to widespread Amazon forest degradation or loss (*7*). The significance of these processes will depend on the growth response of tropical trees to increases in atmospheric carbon dioxide concentration, fire management, and deforestation trends (*3*, *7*). Nevertheless, any shift to drier conditions would favor drought-adapted species, and drier forests store less carbon (*8*). If drought events continue, the era of intact Amazon forests buffering the increase in atmospheric carbon dioxide may have passed.

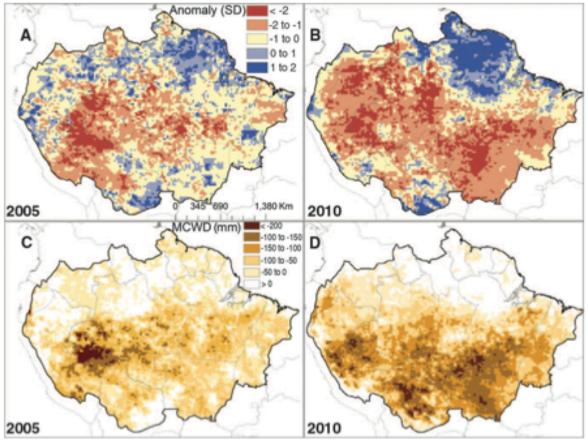

Fig. 1. (**A** and **B**) Satellite-derived standardized anomalies for dry-season rainfall for the two most extensive droughts of the 21st century in Amazonia. (**C** and **D**) The difference in the 12-month (October to September) MCWD from the decadal mean (excluding 2005 and 2010), a measure of drought intensity that correlates with tree mortality. (A) and (C) show the 2005 drought; (B) and (D) show the 2010 drought.

References and Notes

1. Y. Malhi *et al.*, *Science* **319**, 169 (2008); 10.1126/science.1146961.
2. J. A. Marengo *et al.*, *J. Clim.* **21**, 495 (2008).
3. A. Rammig *et al.*, *New Phytol.* **187**, 694 (2010).
4. Material and methods are available as supporting material on *Science* Online.
5. L. E. O. C. Aragão *et al.*, *Geophys. Res. Lett.* **34**, L07701 (2007).
6. O. L. Phillips *et al.*, *Science* **323**, 1344 (2009).
7. S. L. Lewis, *Philos. Trans. R. Soc. London Ser. B* **361**, 195 (2006).
8. E. M. Nogueira, B. W. Nelson, P. M. Fearnside, M. B. França, Á. C. Alves de Oliveira, *For. Ecol. Manage.* **255**, 2963 (2008).

9. We thank T. Baker and L. Aragão for assistance and the Royal Society, Moore Foundation, and NSF for funding.

Supporting Online Material

www.sciencemag.org/cgi/content/full/331/6017/554/DC1
Materials and Methods
Fig. S1
References

23 November 2010; accepted 7 January 2011
10.1126/science.1200807

[1]School of Geography, University of Leeds, Leeds LS2 9JT, UK. [2]Instituto de Pesquisa Ambiental da Amazônia, Avenida Nazaré 669, 66035-170 Belém, Brazil. [3]Woods Hole Research Center, Falmouth, MA 02450, USA. [4]Animal and Plant Sciences, University of Sheffield, Sheffield S10 2TN, UK.

*These authors contributed equally to this manuscript.
†To whom correspondence should be addressed. E-mail: s.l.lewis@leeds.ac.uk

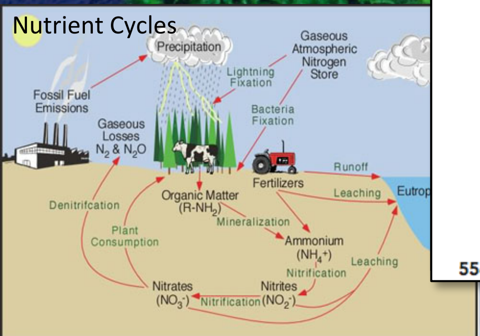

ECOSTRESS

ECOsystem Spaceborne Thermal Radiometer Experiment on Space Station

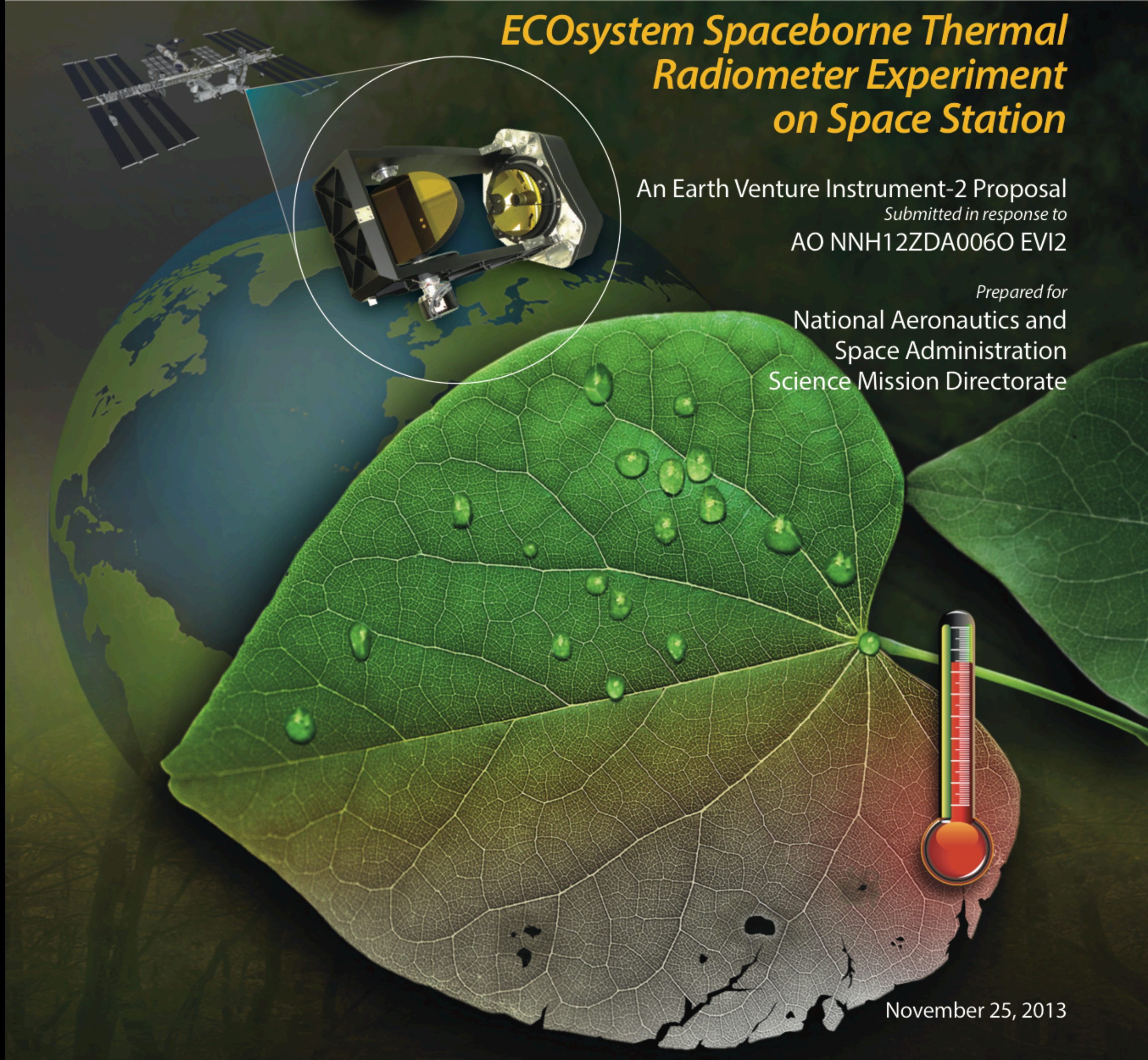

An Earth Venture Instrument-2 Proposal

Submitted in response to

AO NNH12ZDA006O EVI2

Prepared for

National Aeronautics and Space Administration Science Mission Directorate

November 25, 2013